Electronic Supplementary Material (ESI) for Dalton Transactions.

Supporting Information

Diastereoselective Synthesis, Structural and Reactivity Studies of Ferrocenyloxazoline Gold(I) and Gold(II) Complexes

Julia Holz, Marta Ayerbe Garcia, Wolfgang Frey, Felix Krupp, and René Peters*

Institut für Organische Chemie, Universität Stuttgart, Pfaffenwaldring 55, D-70569 Stuttgart, Germany.

Content

NMR Spectra 4

(4*R*,5*S*)-(4,5-5*H*-Indeno[1,2-*d*]-4,5-dihydro-2-oxazolyl) ferrocene (**IndFO**) 4

(4*R*,5*S*,S_p)-(4,5-5*H*-Indeno[1,2-*d*]-4,5-dihydro-2-oxazolyl)-2-methyl ferrocene (**IndFOMe**) 5

(*4R*,5*R*,S_p)-(4,5-Diphenyl-4,5-dihydro-2-oxazolyl)-2-methyl ferrocene (**Ph_2FOMe**) 6

(*S*)-(4-Isopropyl-4,5-dihydro-2-oxazolyl)-2,5-dimethyl ferrocene (***i*PrFOMe$_2$**) 7

(*S*,S_p)-(4-Isopropyl-4,5-dihydro-2-oxazolyl)-2-trimethylsilyl-5-methyl ferrocene (***i*PrFOTMSMe**) 8

(*S*)-(4-*Tert*-butyl-4,5-dihydro-2-oxazolyl)-2,5-dimethyl ferrocene (***t*BuFOMe$_2$**) 9

(4*R*,5*S*)-(4,5-5*H*-Indeno[1,2-*d*]-4,5-dihydro-2-oxazolyl)-2,5-dimethyl ferrocene (**IndFOMe$_2$**) 10

(*4R*,5*R*)-(4,5-Diphenyl-4,5-dihydro-2-oxazolyl)-2,5-dimethyl ferrocene (**Ph_2FOMe$_2$**) 11

Bis[μ-[(η5-(*S*,R_p)-2-(4'-isopropyl-4',5'-dihydro-2'-oxazolyl-κ*N*)-cyclopentadienyl-κ*C*)(η5-cyclopentadienyl) ferrocene]] digold(I) (**(R_p)-*i*PrFOAu(I)**) 12

Bis[μ-[(η5-(*S*,R_p)-2-(4'-isopropyl-4',5'-dihydro-2'-oxazolyl-κ*N*)-3-methyl-cyclopentadienyl-κ*C*)(η5-cyclopentadienyl) ferrocene]] digold(I) (***i*PrFOMeAu(I)**) 13

Bis[μ-[(η^5-(*S*,R_p)-2-(4'-isopropyl-4',5'-dihydro-2'-oxazolyl-κ*N*)-3-trimethylsilyl-cyclopentadienyl-κ*C*)(η^5-cyclopentadienyl) ferrocene]] digold(I) (***i*PrFOTMSAu(I)**) 14

Bis[μ-[(η^5-(*S*,R_p)-2-(4'-*tert*-butyl-4',5'-dihydro-2'-oxazolyl-κ*N*)-3-methyl-cyclopentadienyl-κ*C*)(η^5-cyclopentadienyl) ferrocene]] digold(I) (***t*BuFOMeAu(I)**) 15

Bis[μ-[(η^5-(*S*,S_p)-2-(4',5'-5'*H*-Indeno[1,2-*d*]-4',5'-dihydro-2'-oxazolyl-κ*N*)-3-methyl-cyclopentadienyl-κ*C*)(η^5-cyclopentadienyl) ferrocene]] digold(I) (**IndFOMeAu(I)**) 16

Bis[μ-[(η^5-(*S*,S_p)-2-(4',5'-diphenyl-4',5'-dihydro-2'-oxazolyl-κ*N*)-3-methyl-cyclopentadienyl-κ*C*)(η^5-cyclopentadienyl) ferrocene]] digold(I) (**Ph_2FOMeAu(I)**) 17

rac-Bis[μ-[(η^5-2-(2'-oxazolyl-κ*N*)-3-methyl-cyclopentadienyl-κ*C*)(η^5-cyclopentadienyl) ferrocene]] digold(I) (**H_2FOMeAu(I)**) 18

rac-Bis[μ-[(η^5-2-(4',5'-Dihydro-4',4'-dimethyl-2'-oxazolyl-κ*N*)-3-methyl-cyclopentadienyl-κ*C*)(η^5-cyclopentadienyl) ferrocene]] digold(I) (**Me$_2$FOMeAu(I)**) 19

rac-Bis[μ-[(η^5-2-(2'-oxazolyl-κ*N*)-cyclopentadienyl-κ*C*)(η^5-cyclopentadienyl) ferrocene]] digold(I) (**H_2FOAu(I)**) 20

rac-Bis[μ-[(η^5-2-(4',5'-Dihydro-4',4'-dimethyl-2'-oxazolyl-κ*N*)-cyclopentadienyl-κ*C*)(η^5-cyclopentadienyl) ferrocene]] digold(I) (**Me$_2$FOAu(I)**) 21

Dichlorobis[μ-[(η^5-(*S*,R_p)-2-(4'-isopropyl-4',5'-dihydro-2'-oxazolyl-κ*N*)-3-methyl-cyclopentadienyl-κ*C1*)(η^5-cyclopentadienyl) ferrocene]] digold(II) (***i*PrFOMeAu(II)Cl**) 22

Dichlorobis[μ-[(η^5-(*S*,R_p)-2-(4'-isopropyl-4',5'-dihydro-2'-oxazolyl-κ*N*)-3-trimethylsilyl-cyclopentadienyl-κ*C*)(η^5-cyclopentadienyl) ferrocene]] digold(II) (***i*PrFOTMSAu(II)Cl**) 23

Dichlorobis[μ-[(η^5-(*S*,R_p)-2-(4'-*tert*-butyl-4',5'-dihydro-2'-oxazolyl-κ*N*)-3-methyl-cyclopentadienyl-κ*C*)(η^5-cyclopentadienyl) ferrocene]] digold(II) (***t*BuFOMeAu(II)Cl**) 24

Dichlorobis[μ-[(η^5-(*S*,S_p)-2-(4',5'-5'*H*-Indeno[1,2-*d*]-4',5'-dihydro-2'-oxazolyl-κ*N*)-3-methyl-cyclopentadienyl-κ*C*)(η^5-cyclopentadienyl) ferrocene]] digold(II) (**IndFOMeAu(II)Cl**) 25

Dichlorobis[μ-[(η^5-(*S*,S_p)-2-(4',5'-diphenyl-4',5'-dihydro-2'-oxazolyl-κ*N*)-3-methyl-cyclopentadienyl-κ*C*)(η^5-cyclopentadienyl) ferrocene]] digold(II) (**Ph_2FOMeAu(II)Cl**) 26

Dibromobis[μ-[(η^5-(*S*,R_p)-2-(4'-isopropyl-4',5'-dihydro-2'-oxazolyl-κ*N*)-3-methyl-cyclopentadienyl-κ*C1*)(η^5-cyclopentadienyl) ferrocene]] digold(II) (***i*PrFOMeAu(II)Br**) 27

Diiodobis[μ-[(η^5-(*S*,R_p)-2-(4'-isopropyl-4',5'-dihydro-2'-oxazolyl-κ*N*)-3-methyl-cyclopentadienyl-κ*C1*)(η^5-cyclopentadienyl) ferrocene]] digold(II) (***i*PrFOMeAu(II)I**) 28

(*S*,R_p,*S*,R_p)-2,2'-Bis[(4-Isopropyl-4,5-dihydro-2-oxazolyl)-3-methyl] 1,1'-biferrocenyl (**(*i*PrFOMe)$_2$**) 29

Diacetatobis[μ-[(η^5-(*S*,R_p)-2-(4'-isopropyl-4',5'-dihydro-2'-oxazolyl-κ*N*)-3-methyl-cyclopentadienyl-κ*C1*)(η^5-cyclopentadienyl) ferrocene]] digold(II) (***i*PrFOMeAu(II)OAc**) 30

UV-Vis Spectra 31

CD Spectra 32

NMR Spectra

(4*R*,5*S*)-(4,5-5*H*-Indeno[1,2-*d*]-4,5-dihydro-2-oxazolyl) ferrocene (IndFO)

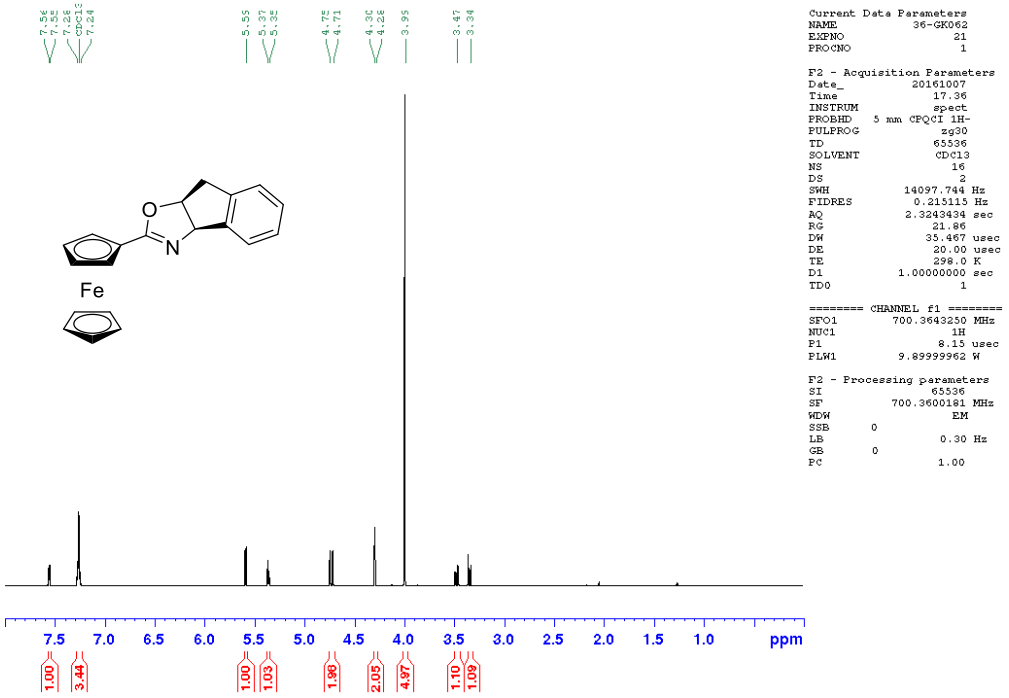

Figure S1m ^{1}H NMR spectrum at 700 MHz of Compound **IndFO** in $CDCl_3$.

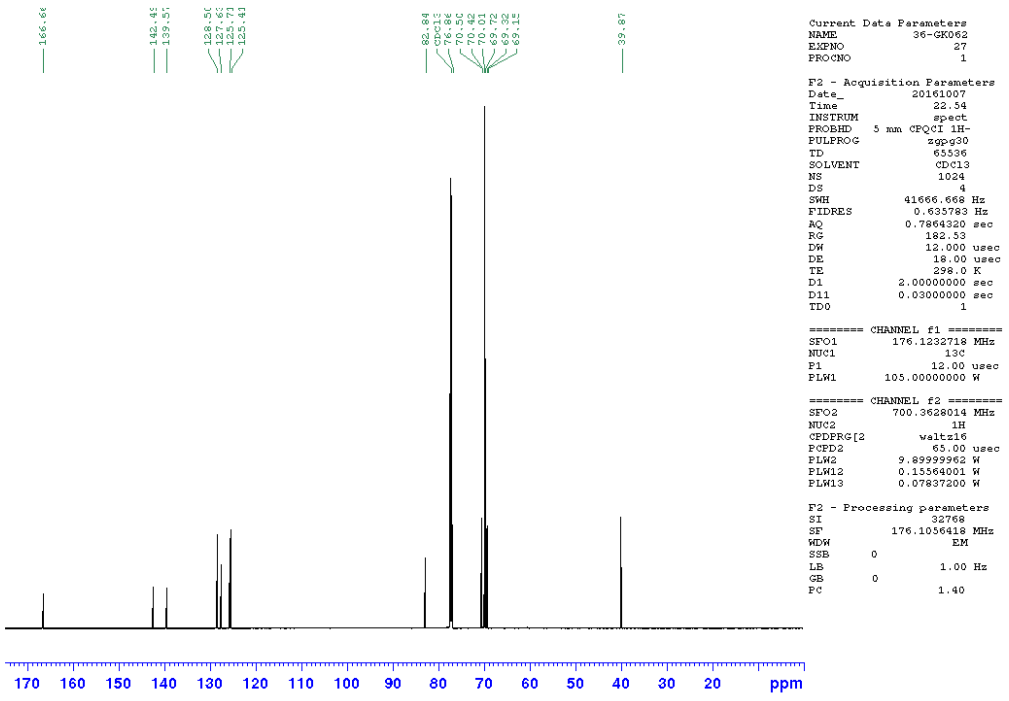

Figure S2 ^{13}C {^{1}H} NMR spectrum at 175 MHz of Compound **IndFO** in $CDCl_3$.

(4*R*,5*S*,S_p)-(4,5-5*H*-Indeno[1,2-*d*]-4,5-dihydro-2-oxazolyl)-2-methyl ferrocene (IndFOMe)

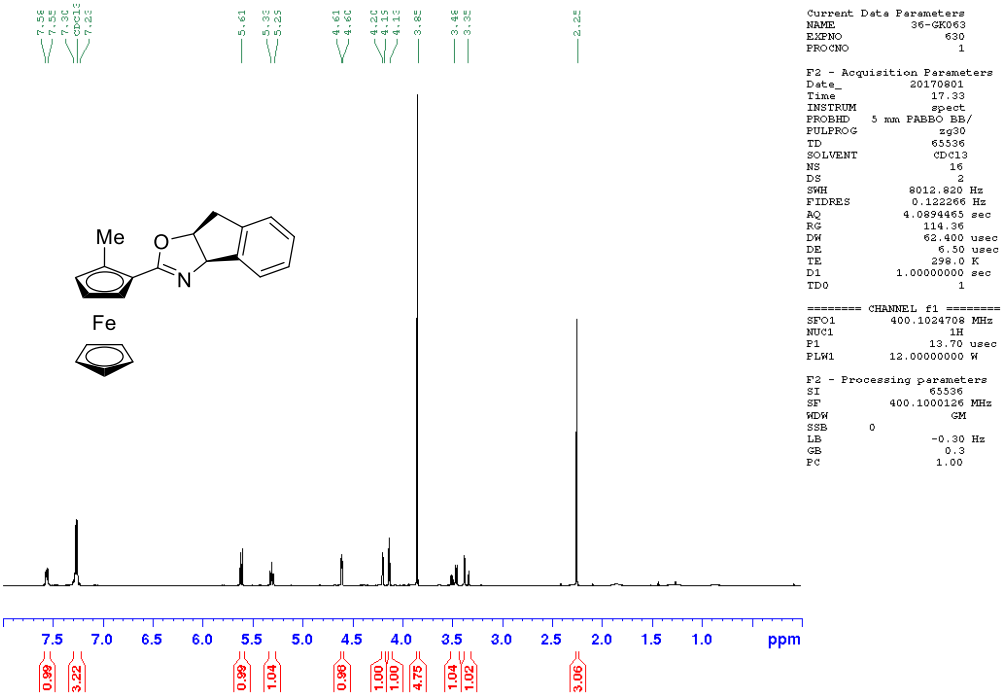

Figure S3 ^{1}H NMR spectrum at 400 MHz of Compound **IndFOMe** in $CDCl_3$.

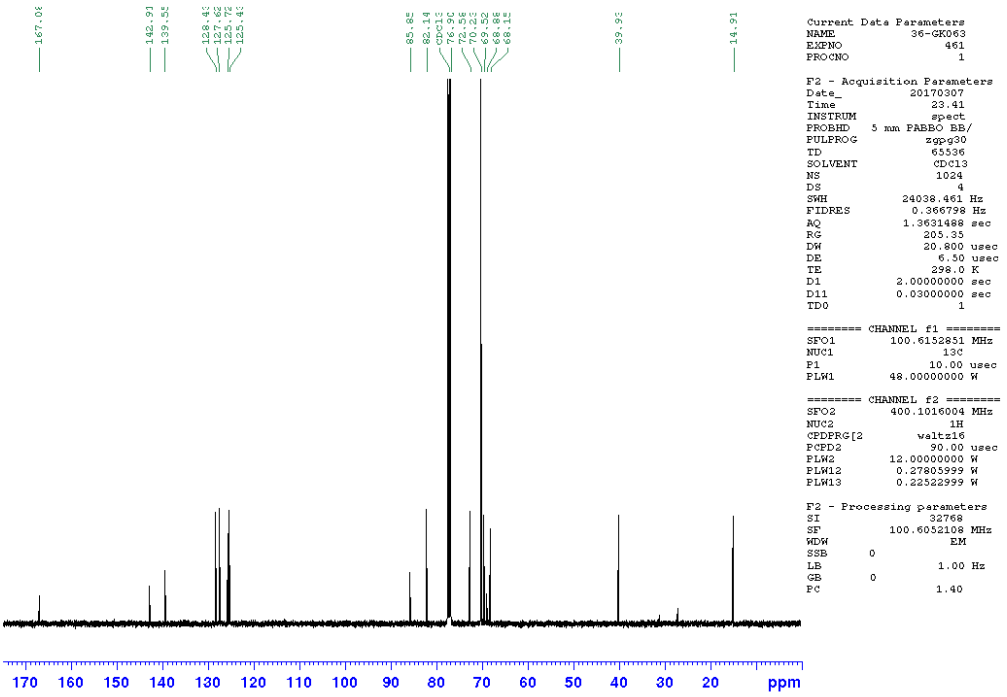

Figure S4 ^{13}C {^{1}H} NMR spectrum at 100 MHz of Compound **IndFOMe** in $CDCl_3$.

(*4R*,5*R*,*S*$_p$)-(4,5-Diphenyl-4,5-dihydro-2-oxazolyl)-2-methyl ferrocene (Ph_2FOMe)

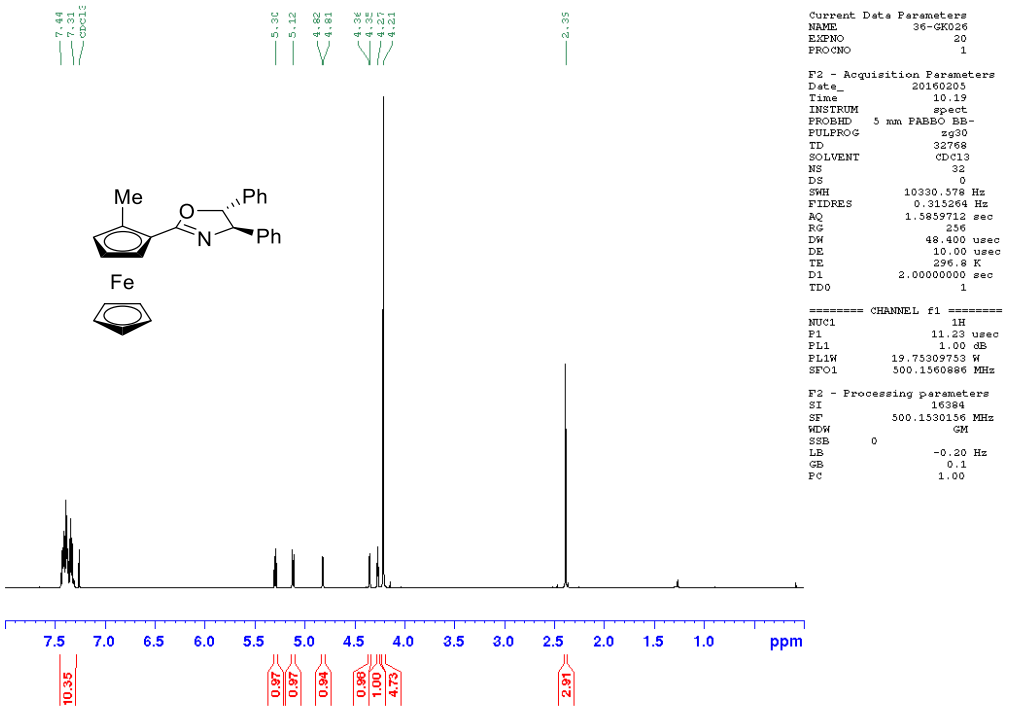

Figure S5 ^{1}H NMR spectrum at 500 MHz of Compound **Ph_2FOMe** in $CDCl_3$.

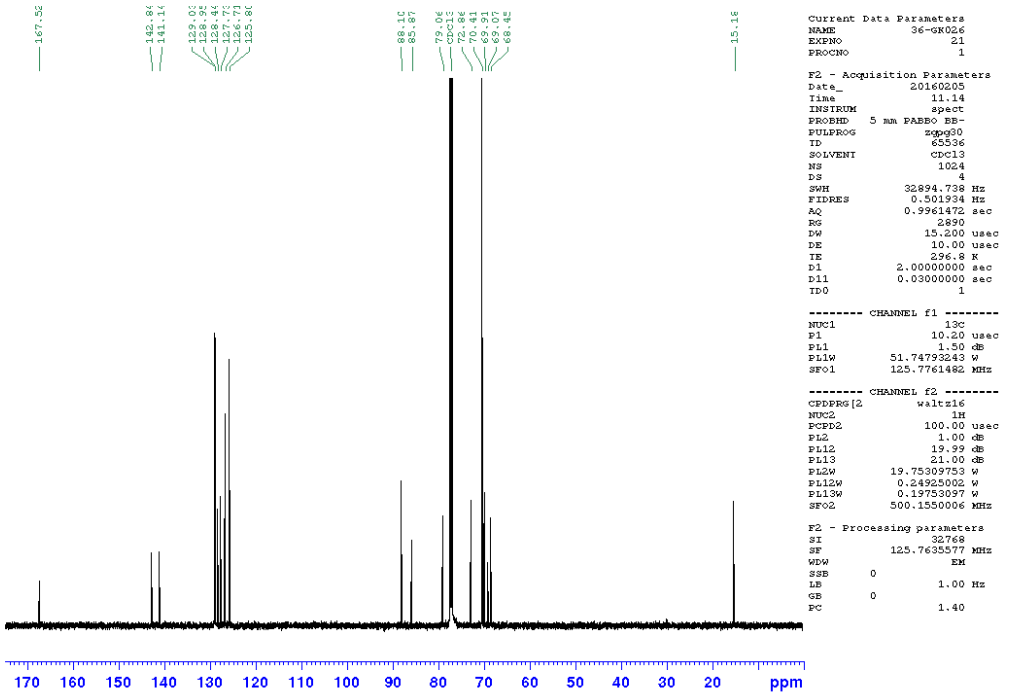

Figure S6 ^{13}C {^{1}H} NMR spectrum at 125 MHz of Compound **Ph_2FOMe** in $CDCl_3$.

(*S*)-(4-Isopropyl-4,5-dihydro-2-oxazolyl)-2,5-dimethyl ferrocene (*i*PrFOMe$_2$)

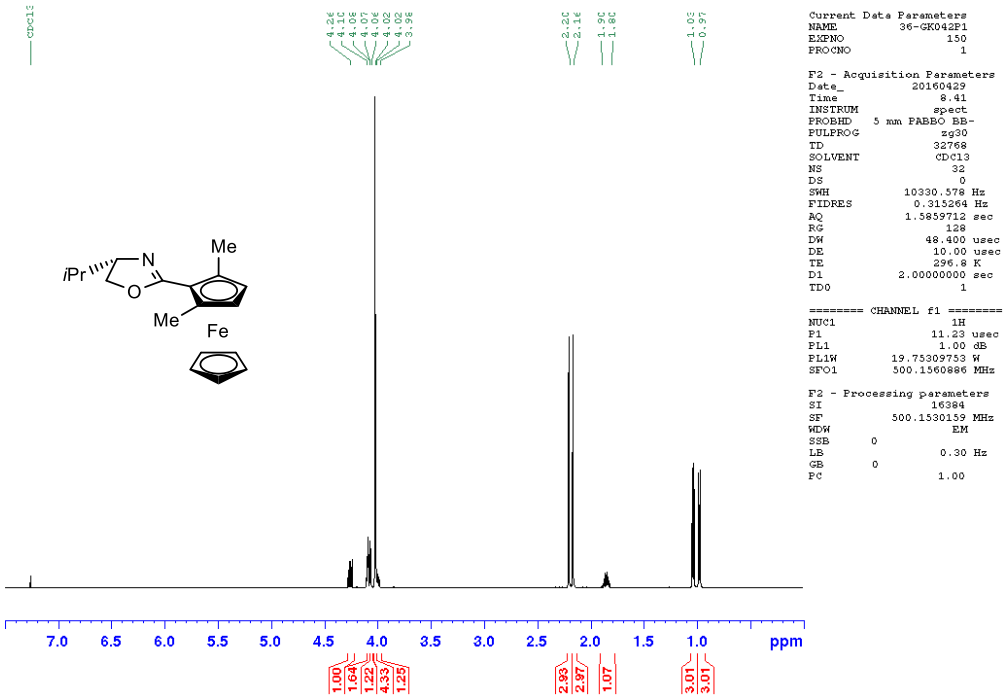

Figure S7 ^{1}H NMR spectrum at 500 MHz of Compound ***i*PrFOMe$_2$** in $CDCl_3$.

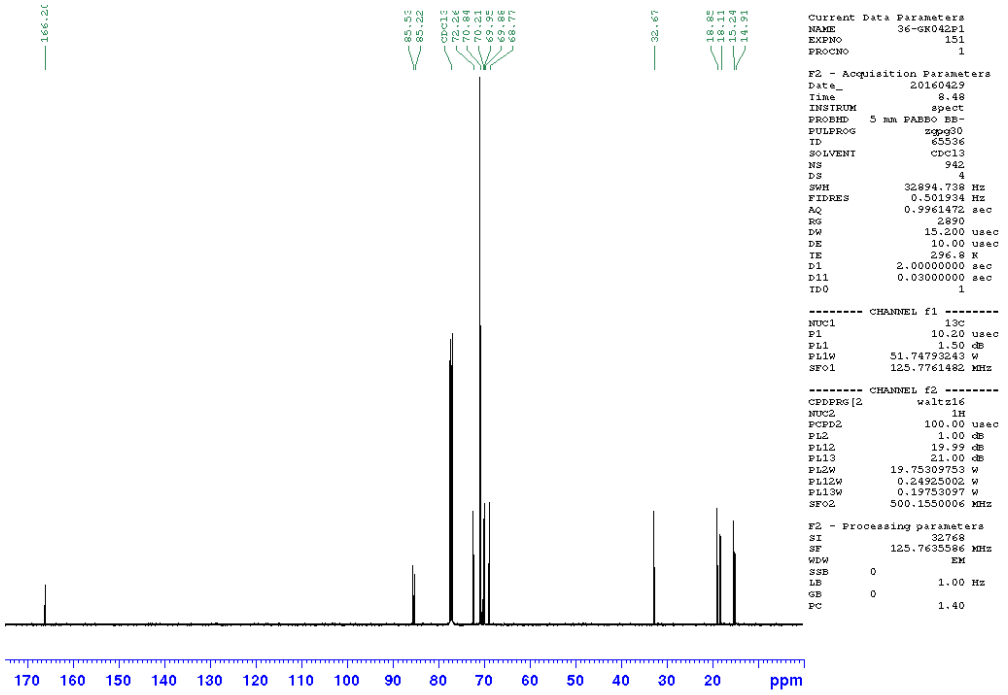

Figure S8 ^{13}C {^{1}H} NMR spectrum at 125 MHz of Compound ***i*PrFOMe$_2$** in $CDCl_3$.

(S,S_p)-(4-Isopropyl-4,5-dihydro-2-oxazolyl)-2-trimethylsilyl-5-methyl ferrocene (*i*PrFOTMSMe)

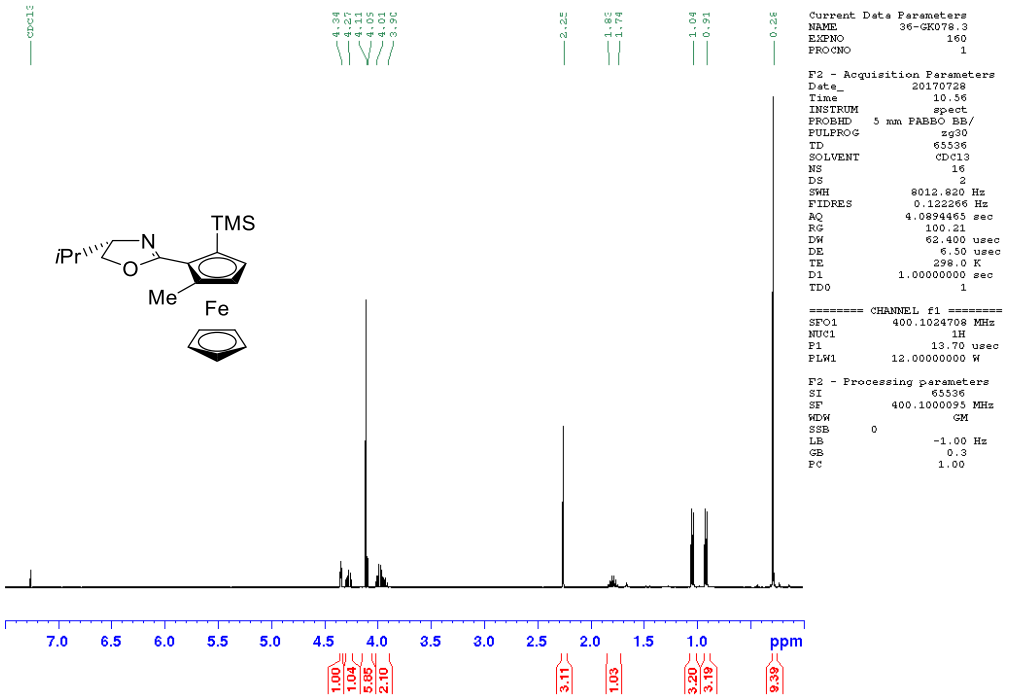

Figure S9 ^{1}H NMR spectrum at 400 MHz of Compound ***i*PrFOTMSMe** in $CDCl_3$.

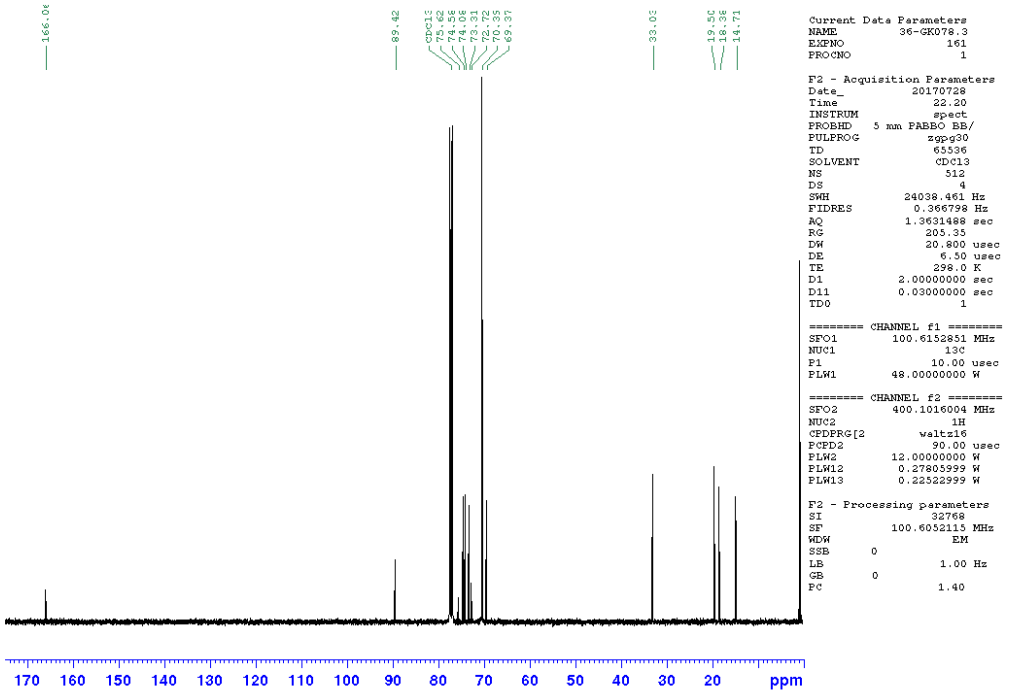

Figure S10 ^{13}C {^{1}H} NMR spectrum at 100 MHz of Compound ***i*PrFOTMSMe** in $CDCl_3$.

(*S*)-(4-*Tert*-butyl-4,5-dihydro-2-oxazolyl)-2,5-dimethyl ferrocene (*t*BuFOMe$_2$)

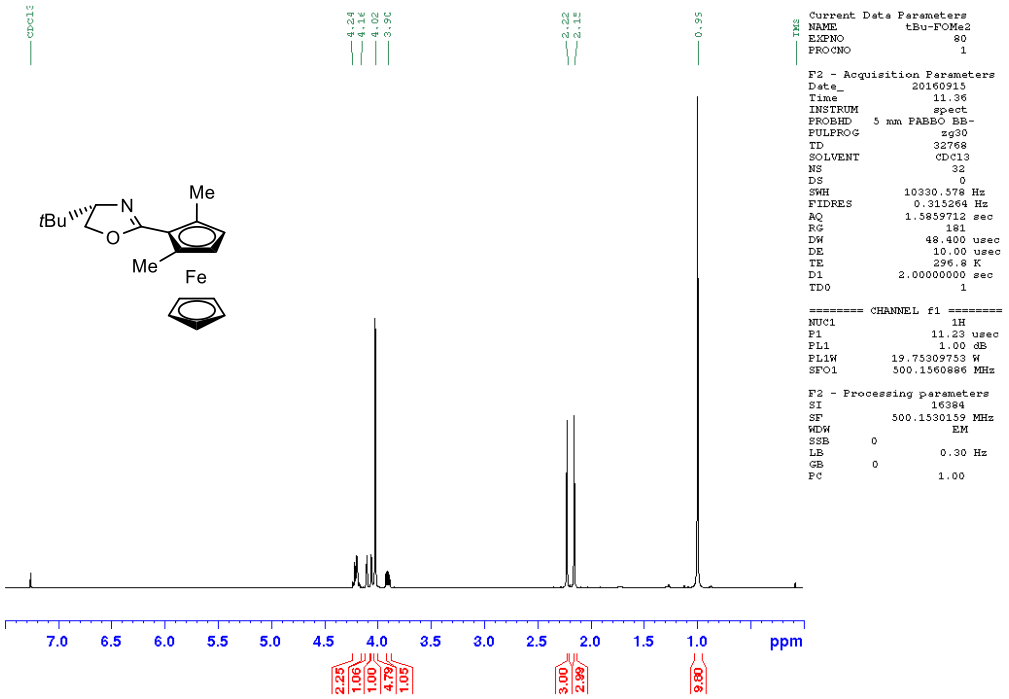

Figure S11 ^{1}H NMR spectrum at 500 MHz of Compound ***t*BuFOMe$_2$** in $CDCl_3$.

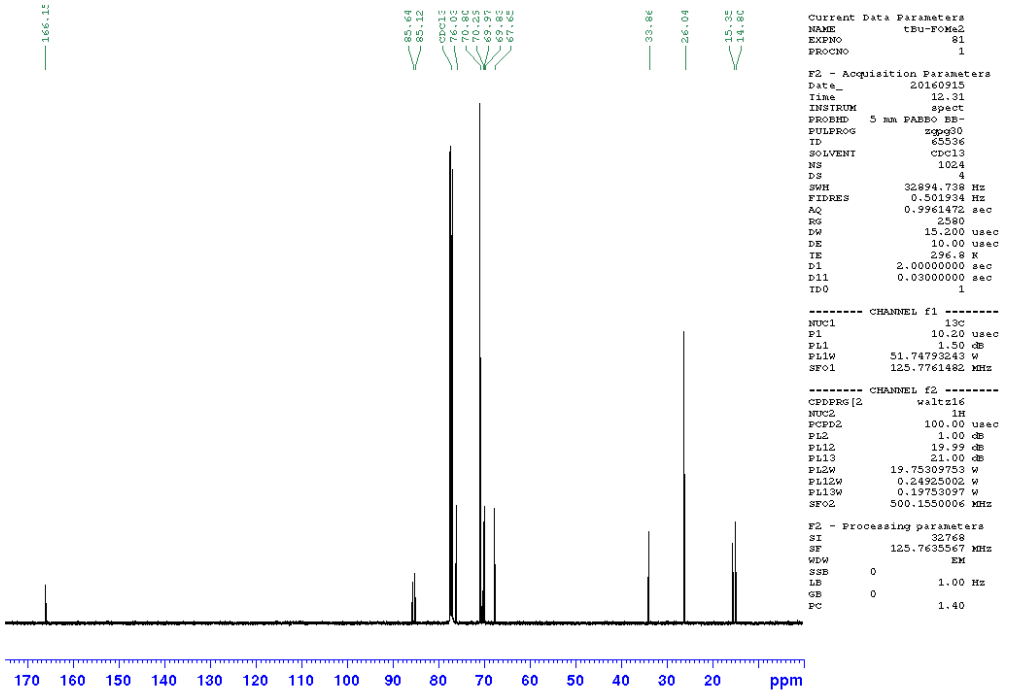

Figure S12 ^{13}C {^{1}H} NMR spectrum at 125 MHz of Compound ***t*BuFOMe$_2$** in $CDCl_3$.

(4*R*,5*S*)-(4,5-5*H*-Indeno[1,2-*d*]-4,5-dihydro-2-oxazolyl)-2,5-dimethyl ferrocene (IndFOMe$_2$)

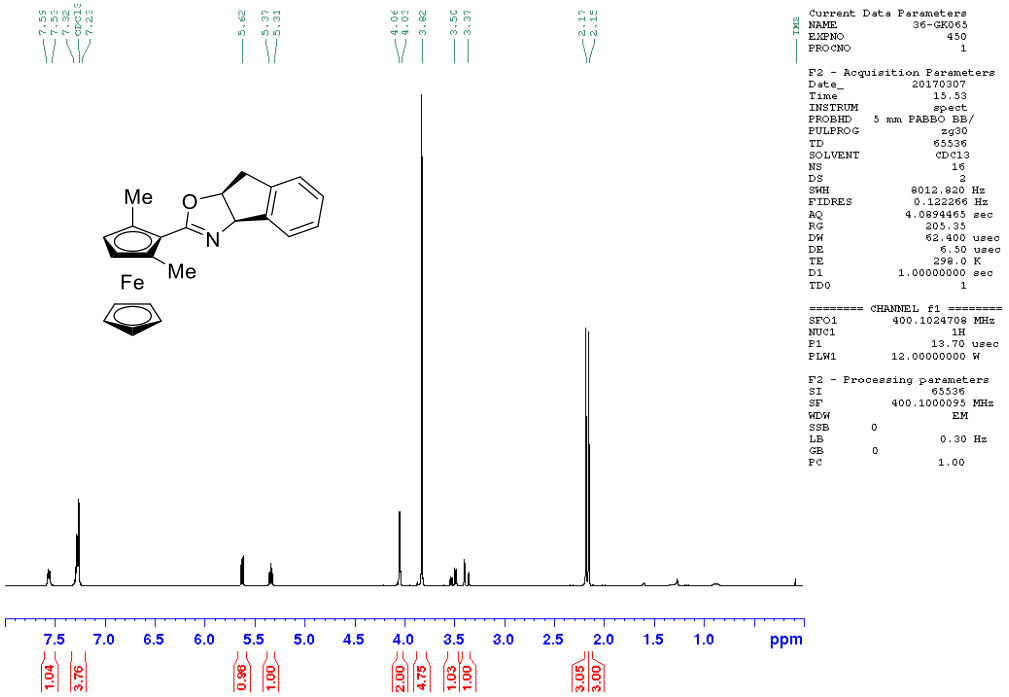

Figure S13 ^{1}H NMR spectrum at 400 MHz of Compound **IndFOMe$_2$** in $CDCl_3$.

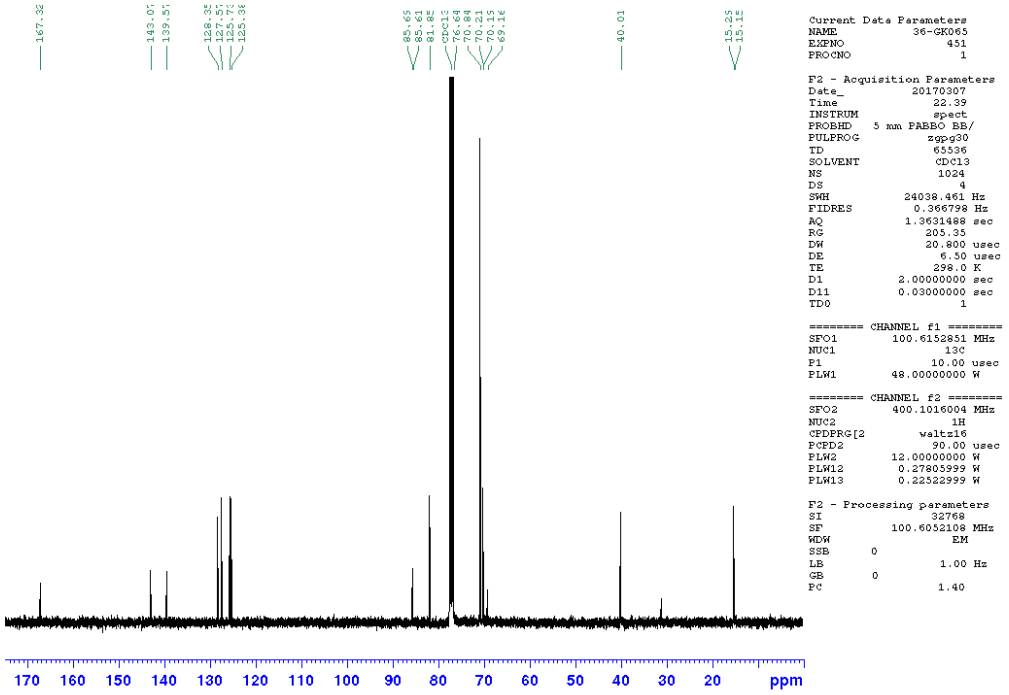

Figure S14 ^{13}C {^{1}H} NMR spectrum at 100 MHz of Compound **IndFOMe$_2$** in $CDCl_3$.

(*4R*,5*R*)-(4,5-Diphenyl-4,5-dihydro-2-oxazolyl)-2,5-dimethyl ferrocene (Ph_2FOMe_2)

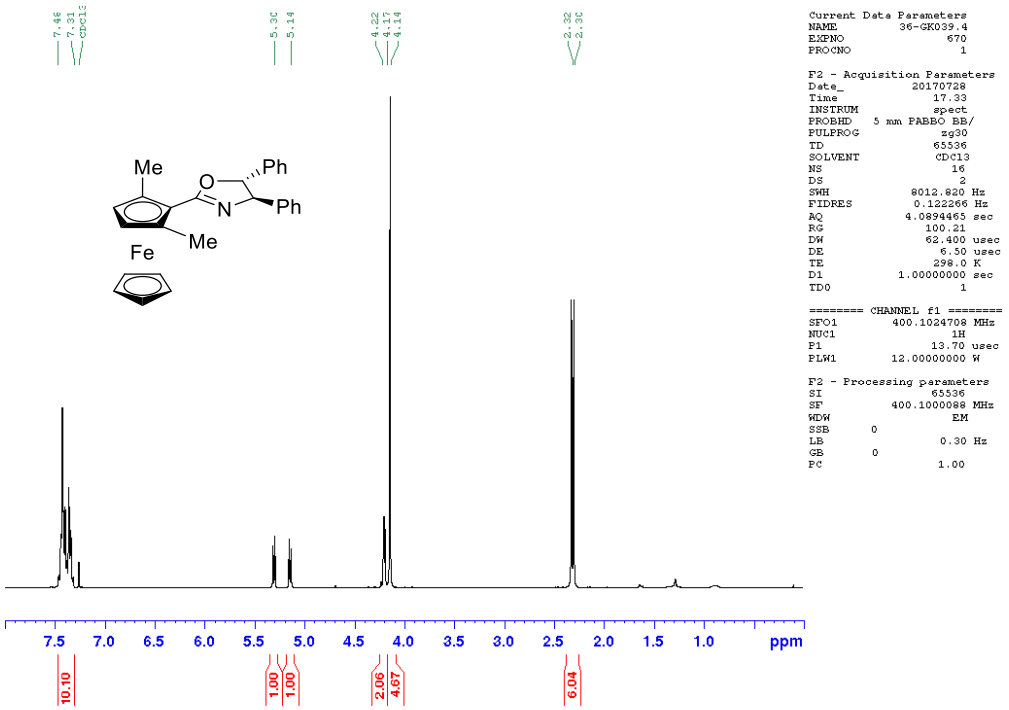

Figure S15 ^{1}H NMR spectrum at 400 MHz of Compound **Ph_2FOMe_2** in $CDCl_3$.

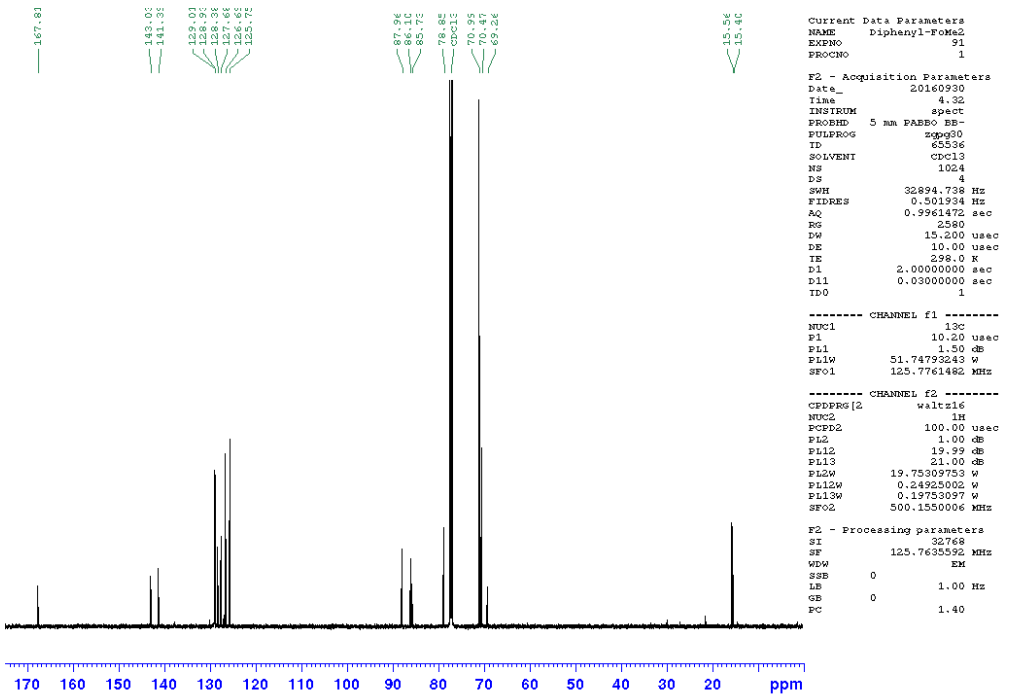

Figure S16 ^{13}C {^{1}H} NMR spectrum at 125 MHz of Compound **Ph_2FOMe_2** in $CDCl_3$.

Bis[μ-[(η5-(*S*,R_p)-2-(4'-isopropyl-4',5'-dihydro-2'-oxazolyl-κ*N*)-cyclopentadienyl-κ*C*)(η5-cyclopentadienyl) ferrocene]] digold(I) ((*R*$_p$)-*i*PrFOAu(I))

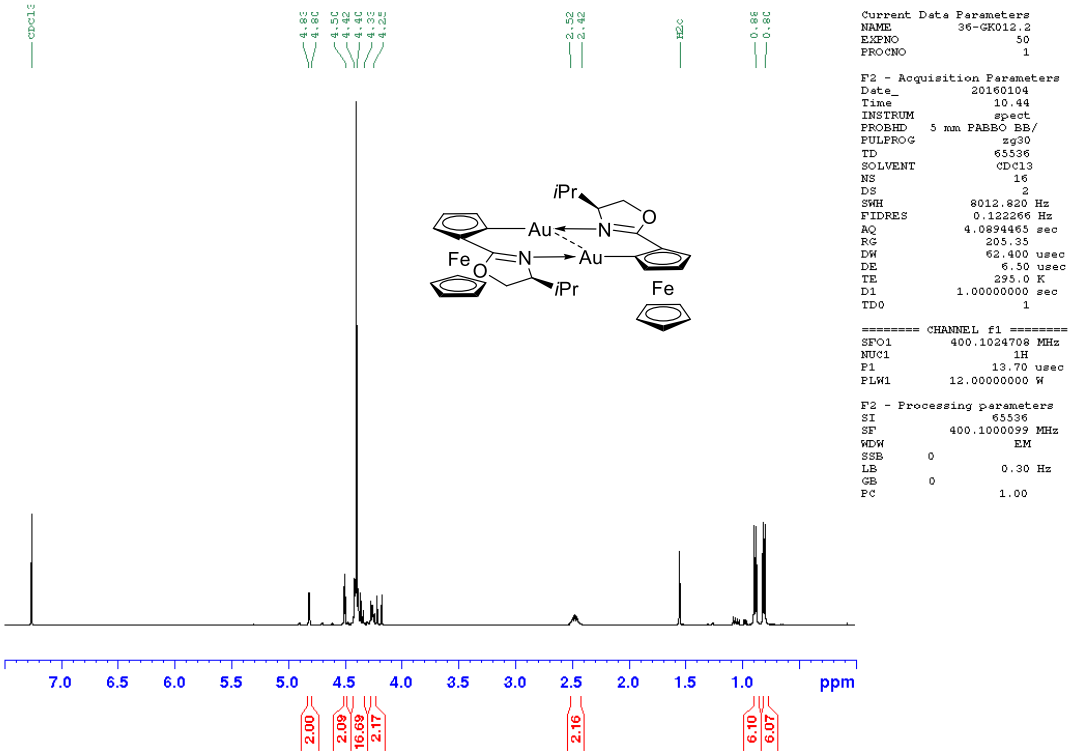

Figure S17 ^{1}H NMR spectrum at 400 MHz of Compound **(*R*$_p$)-*i*PrFOAu(I)** in $CDCl_3$.

Bis[μ-[(η5-(*S*,R_p)-2-(4'-isopropyl-4',5'-dihydro-2'-oxazolyl-κ*N*)-3-methyl-cyclopentadienyl-κ*C*)(η5-cyclopentadienyl) ferrocene]] digold(I) (*i*PrFOMeAu(I))

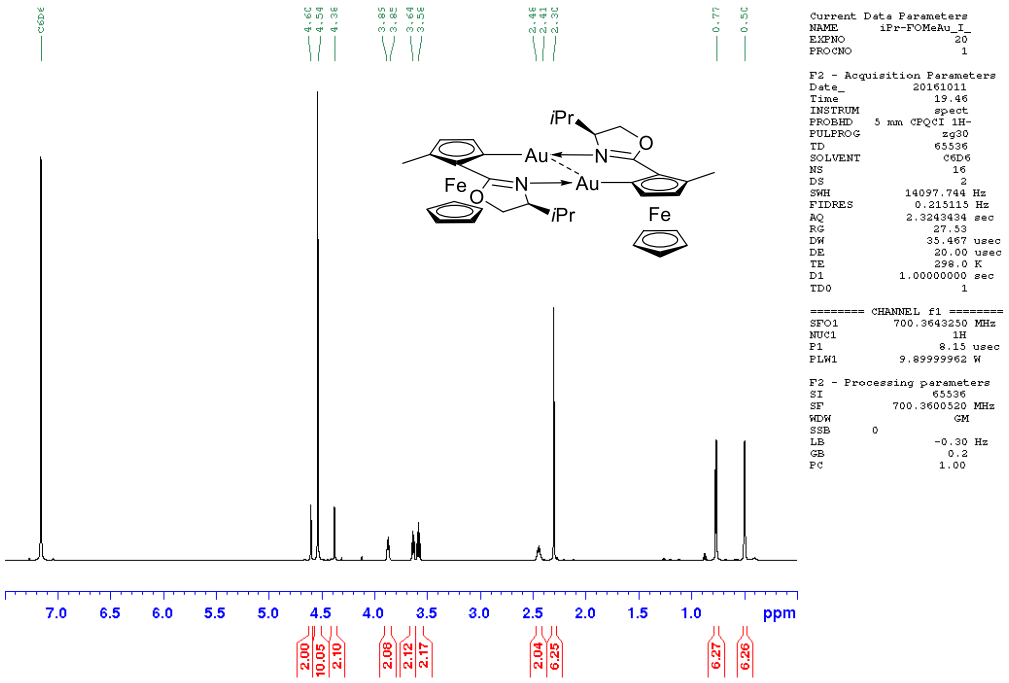

Figure S18 ^{1}H NMR spectrum at 700 MHz of Compound ***i*PrFOMeAu(I)** in C_6D_6.

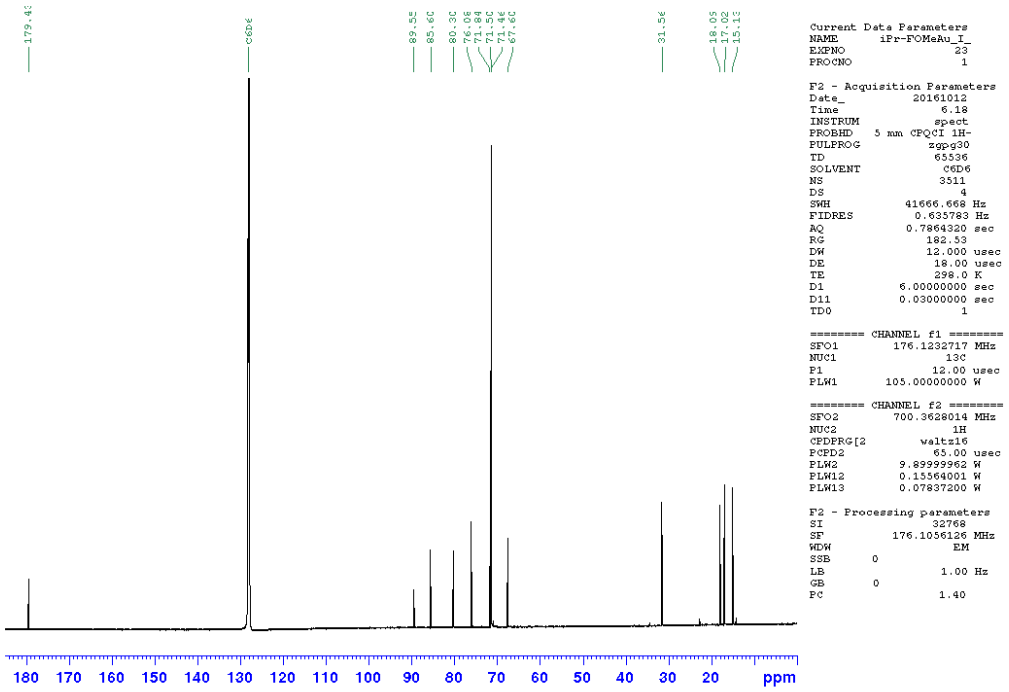

Figure S19 ^{13}C {^{1}H} NMR spectrum at 175 MHz of Compound ***i*PrFOMeAu(I)** in C_6D_6.

Bis[μ-[(η^5-(*S*,*R*$_p$)-2-(4'-isopropyl-4',5'-dihydro-2'-oxazolyl-κ*N*)-3-trimethylsilyl-cyclopentadienyl-κ*C*)(η^5-cyclopentadienyl) ferrocene]] digold(I) (*i*PrFOTMSAu(I))

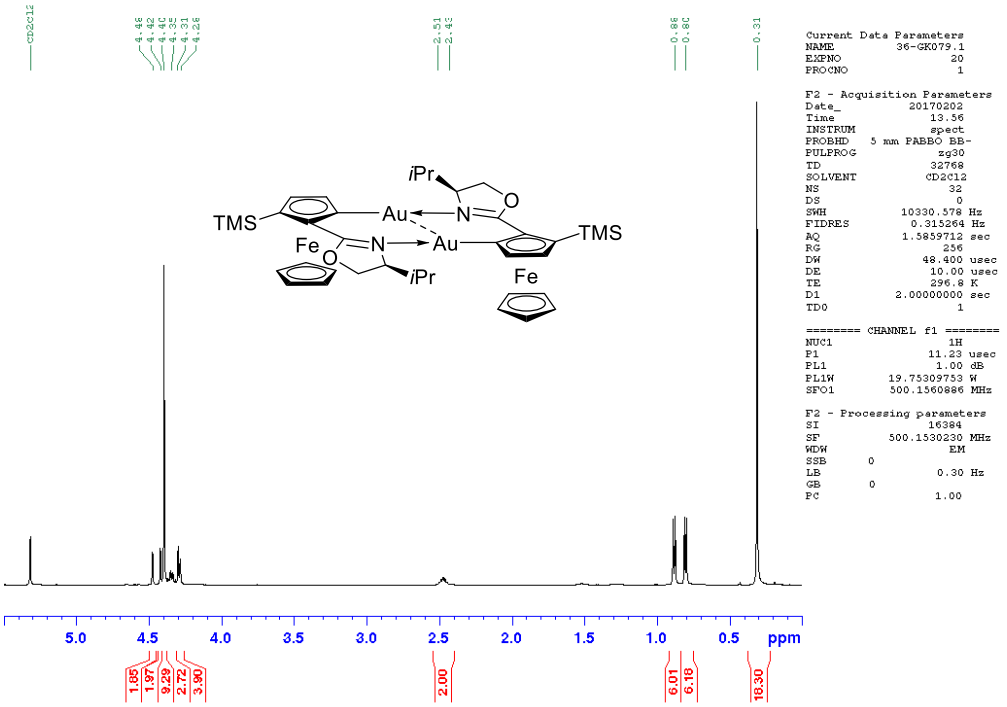

Figure S20 ^{1}H NMR spectrum at 500 MHz of Compound ***i*PrFOTMSAu(I)** in CD_2Cl_2.

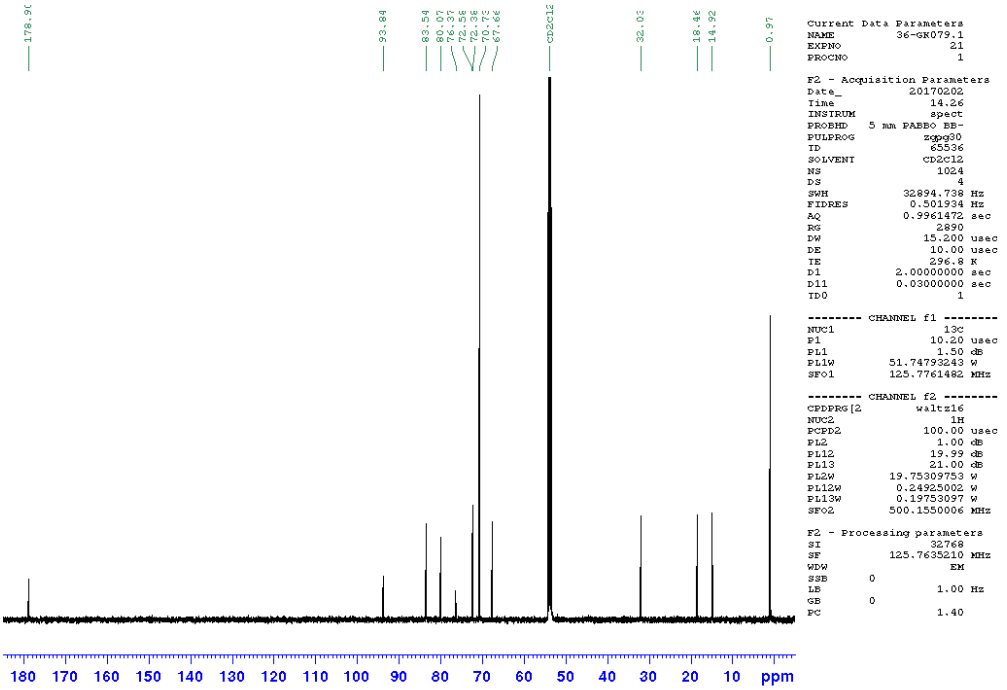

Figure S21 ^{13}C {^{1}H} NMR spectrum at 125 MHz of Compound ***i*PrFOTMSAu(I)** in CD_2Cl_2.

Bis[μ-[(η^5-(*S*,*R*$_p$)-2-(4'-*tert*-butyl-4',5'-dihydro-2'-oxazolyl-κ*N*)-3-methyl-cyclopentadienyl-κ*C*)(η^5-cyclopentadienyl) ferrocene]] digold(I) (*t*BuFOMeAu(I))

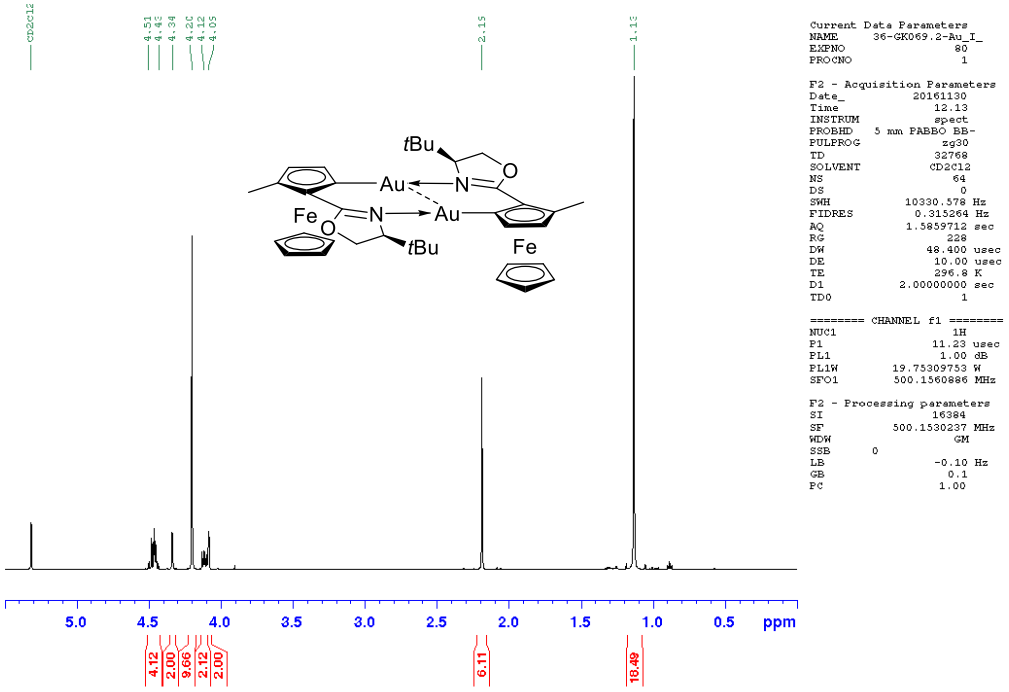

Figure S22 ^{1}H NMR spectrum at 500 MHz of Compound ***t*BuFOMeAu(I)** in CD_2Cl_2.

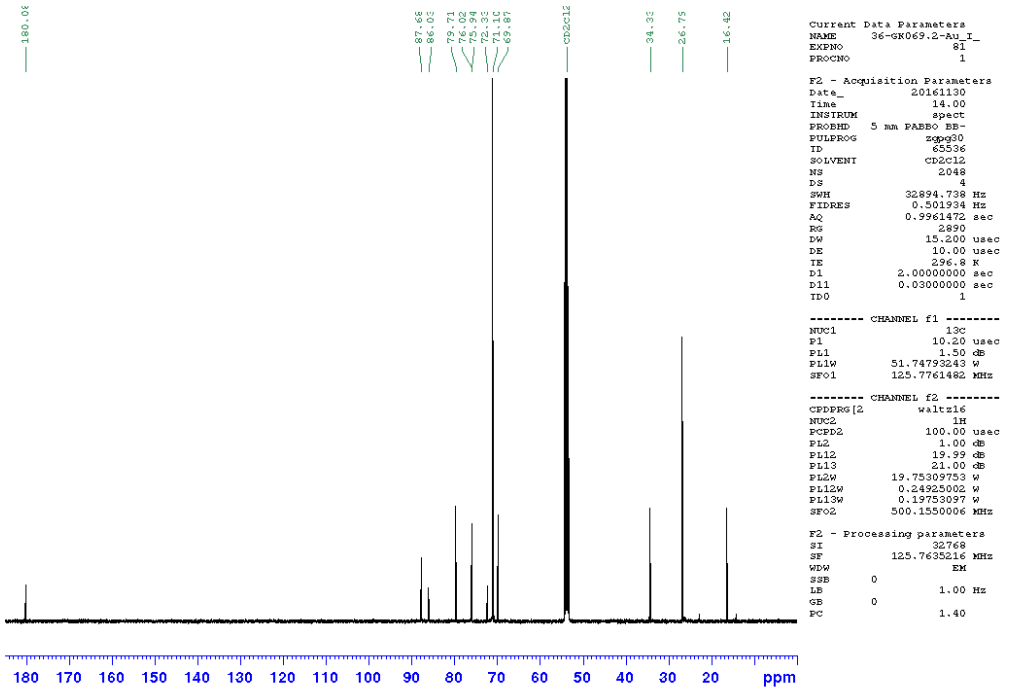

Figure S23 ^{13}C {^{1}H} NMR spectrum at 125 MHz of Compound ***t*BuFOMeAu(I)** in CD_2Cl_2.

Bis[μ-[(η^5-(*S*,*S*$_p$)-2-(4',5'-5'*H*-Indeno[1,2-*d*]-4',5'-dihydro-2'-oxazolyl-κ*N*)-3-methyl-cyclopentadienyl-κ*C*)(η^5-cyclopentadienyl) ferrocene]] digold(I) (IndFOMeAu(I))

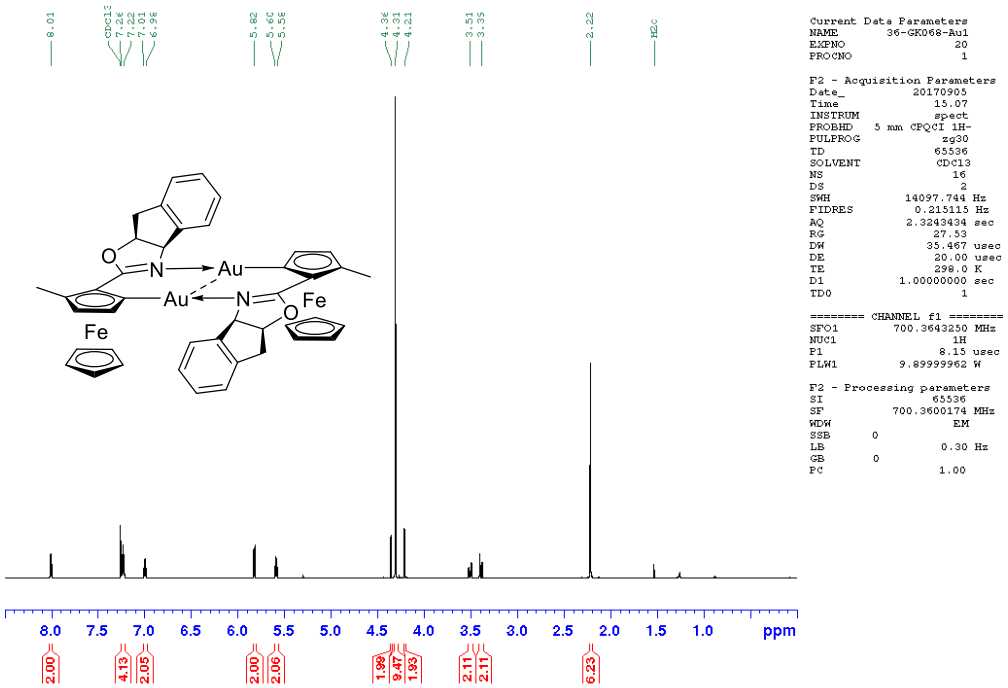

Figure S24 ^{1}H NMR spectrum at 700 MHz of Compound **IndFOMeAu(I)** in $CDCl_3$.

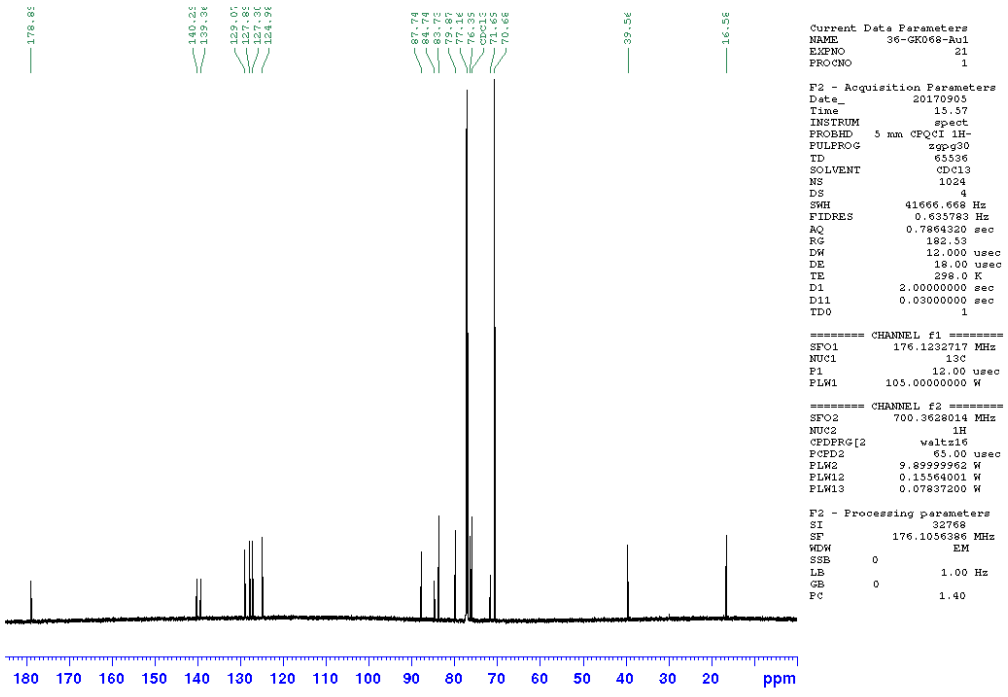

Figure S25 ^{13}C {^{1}H} NMR spectrum at 175 MHz of Compound **IndFOMeAu(I)** in $CDCl_3$.

Bis[μ-[(η^5-(*S*,*S*$_p$)-2-(4',5'-diphenyl-4',5'-dihydro-2'-oxazolyl-κ*N*)-3-methyl-cyclopentadienyl-κ*C*)(η^5-cyclopentadienyl) ferrocene]] digold(I) (Ph$_2$FOMeAu(I))

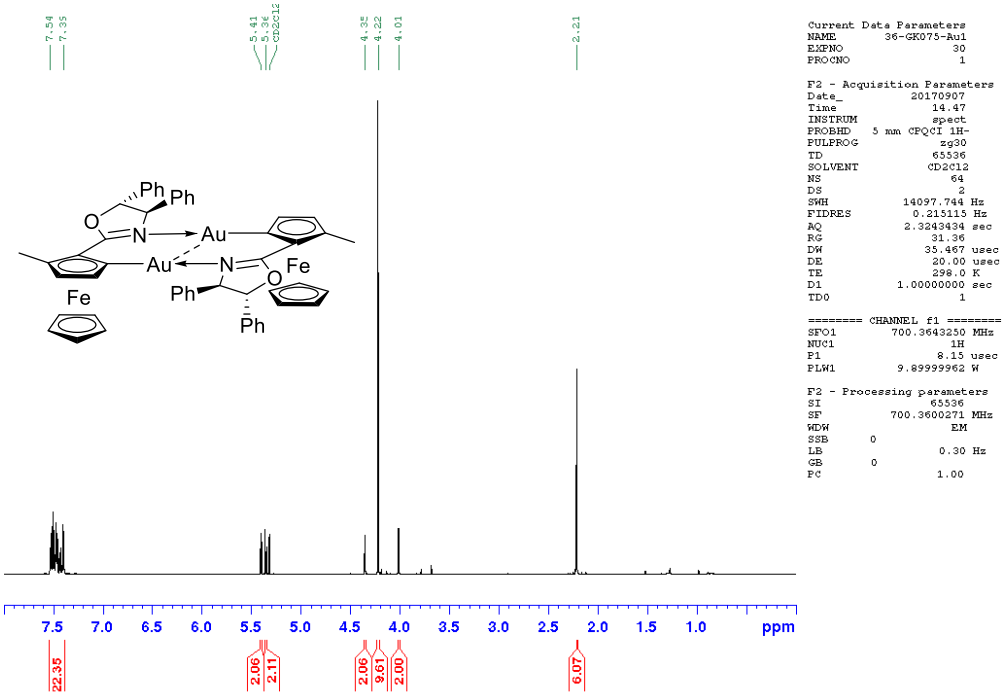

Figure S26 ^{1}H NMR spectrum at 700 MHz of Compound **Ph$_2$FOMeAu(I)** in CD_2Cl_2.

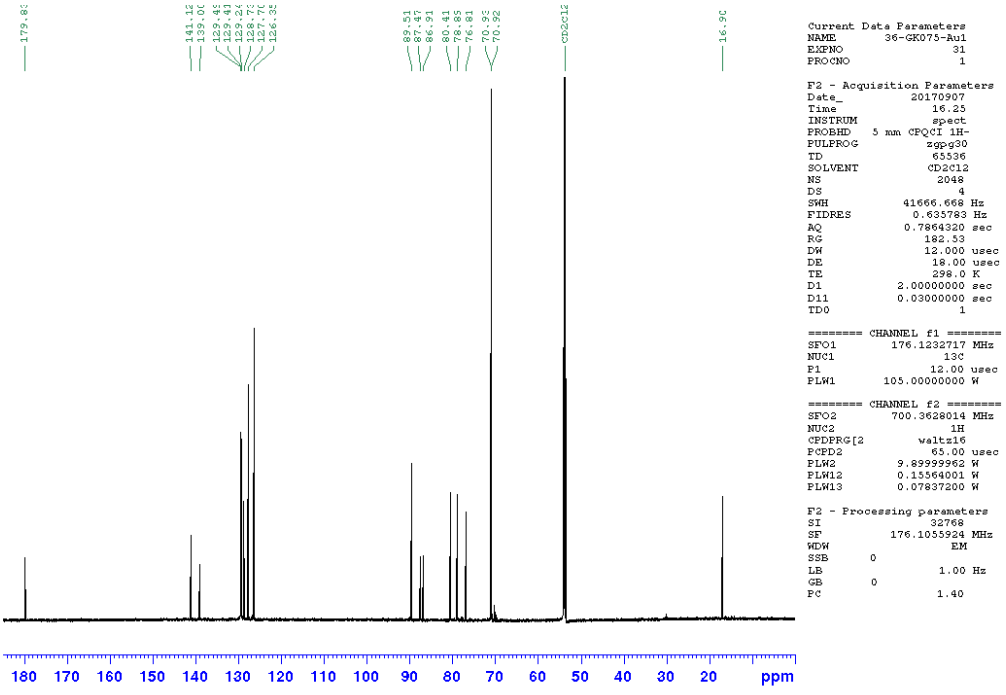

Figure S27 ^{13}C {^{1}H} NMR spectrum at 175 MHz of Compound **Ph$_2$FOMeAu(I)** in CD_2Cl_2.

rac-Bis[μ-[(η^5-2-(2'-oxazolyl-κ*N*)-3-methyl-cyclopentadienyl-κ*C*)(η^5-cyclopentadienyl) ferrocene]] digold(I) (H_2FOMeAu(I))

Due to fast decomposition the NMR spectra are not perfectly pure and an absolute proof of purity was not possible. Especially the ^{1}H-NMR is quite complex.

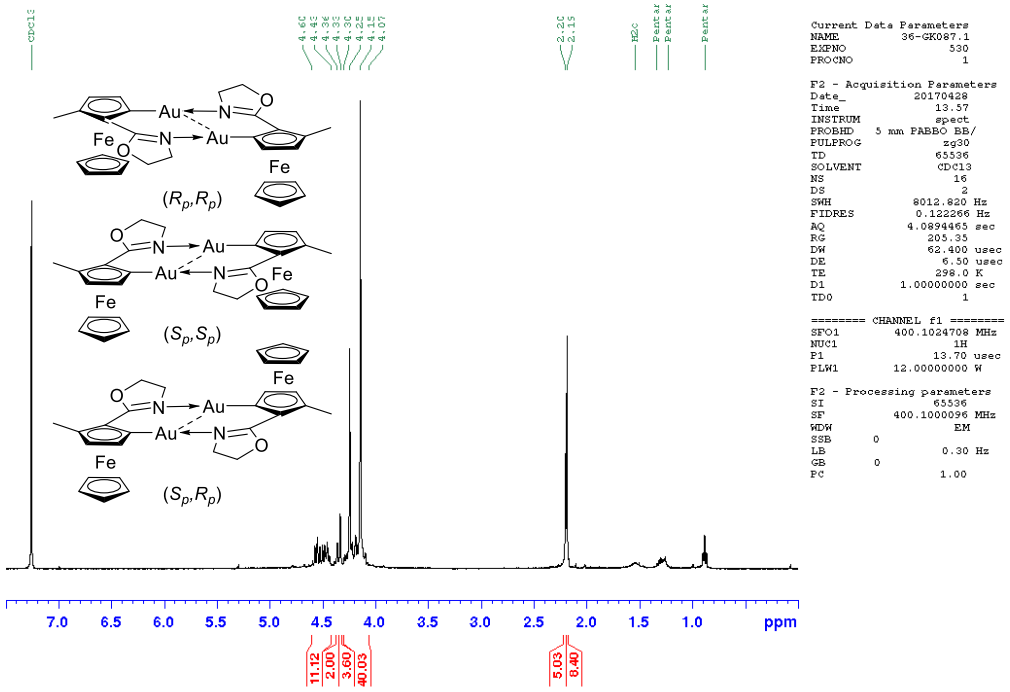

Figure S28 ^{1}H NMR spectrum at 400 MHz of Compound **H_2FOMeAu(I)** in $CDCl_3$.

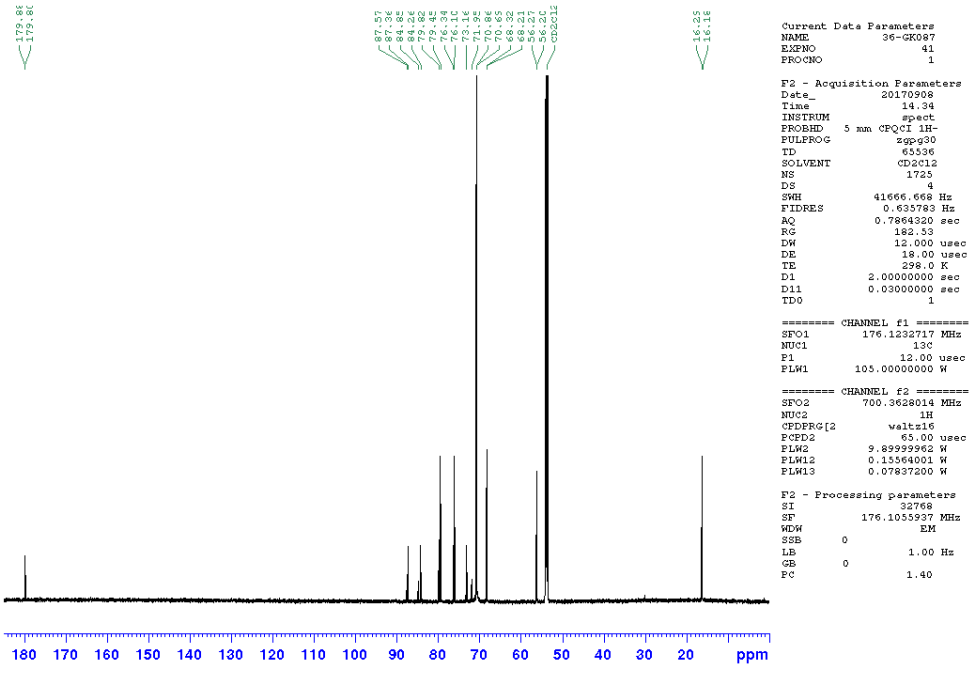

Figure S29 ^{13}C {^{1}H} NMR spectrum at 175 MHz of Compound **H_2FOMeAu(I)** in CD_2Cl_2.

***rac*-Bis[μ-[(η^5-2-(4',5'-Dihydro-4',4'-dimethyl-2'-oxazolyl-κ*N*)-3-methyl-cyclopentadienyl-κ*C*)(η^5-cyclopentadienyl) ferrocene]] digold(I) (Me_2FOMeAu(I))**

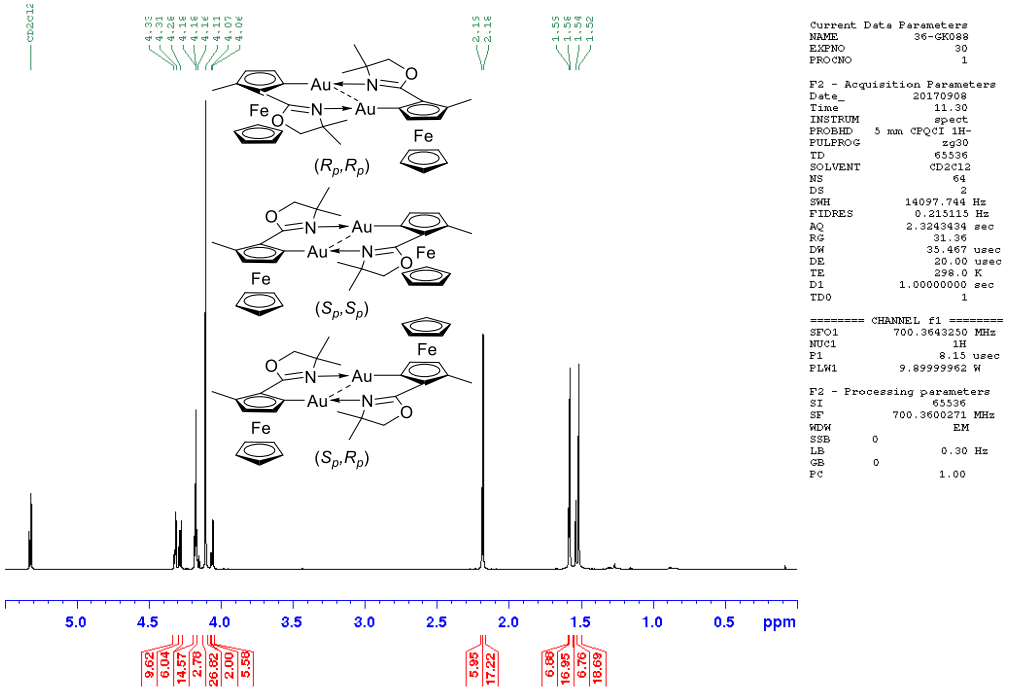

Figure S30 ^{1}H NMR spectrum at 700 MHz of Compound **Me_2FOMeAu(I)** in CD_2Cl_2.

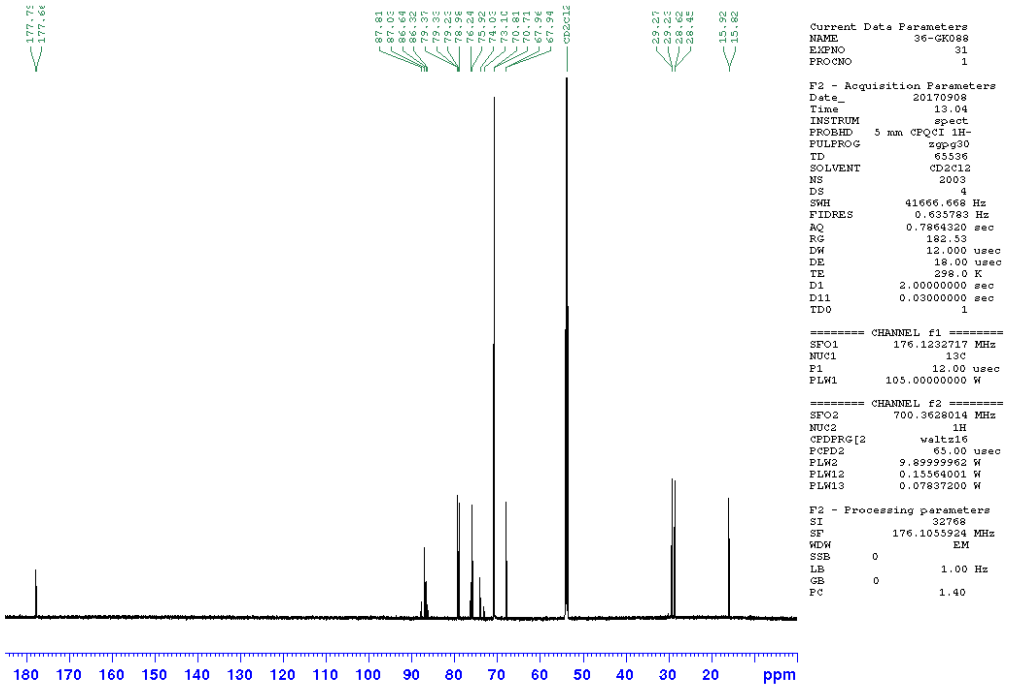

Figure S31 ^{13}C {^{1}H} NMR spectrum at 175 MHz of Compound **Me_2FOMeAu(I)** in CD_2Cl_2.

rac-Bis[μ-[(η^5-2-(2'-oxazolyl-κ*N*)-cyclopentadienyl-κ*C*)(η^5-cyclopentadienyl) ferrocene]] digold(I) (H_2FOAu(I))

Due to fast decomposition the NMR spectra are not perfectly pure and an absolute proof of purity was not possible.

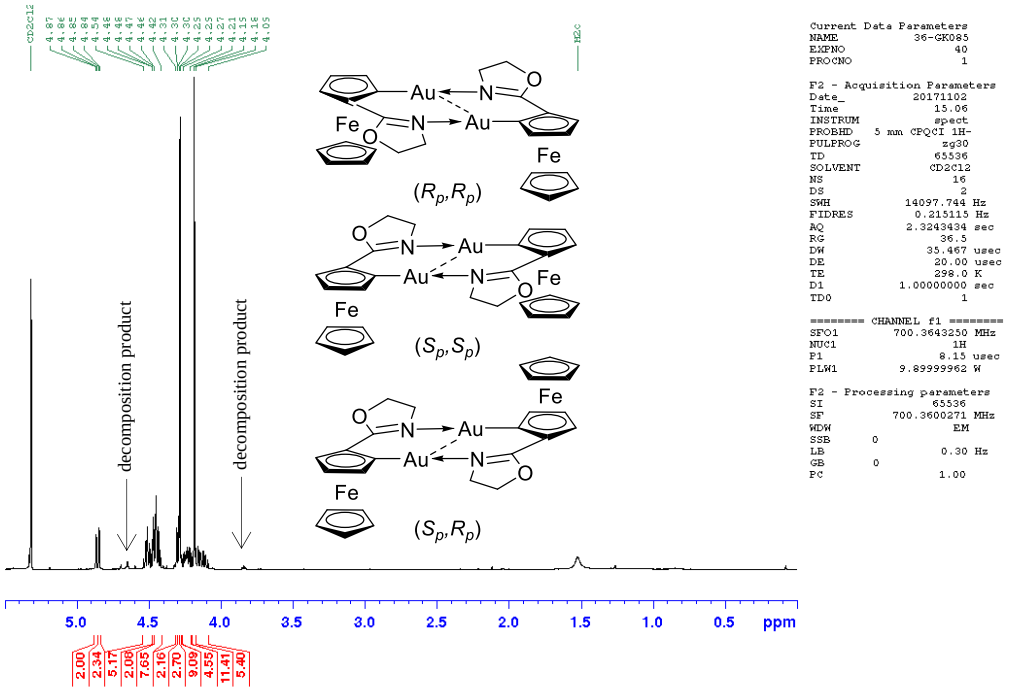

Figure S32 ^{1}H NMR spectrum at 700 MHz of Compound **H_2FOAu(I)** in CD_2Cl_2.

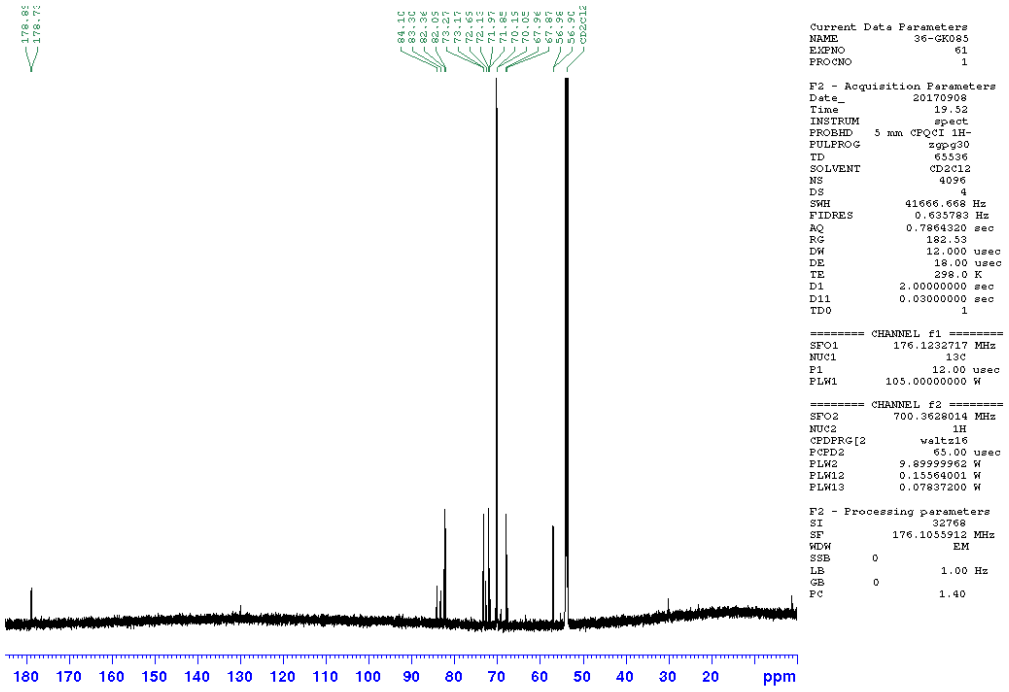

Figure S33 ^{13}C {^{1}H} NMR spectrum at 175 MHz of Compound **H_2FOAu(I)** in CD_2Cl_2.

***rac*-Bis[μ-[(η^5-2-(4',5'-Dihydro-4',4'-dimethyl-2'-oxazolyl-κ*N*)-cyclopentadienyl-κ*C*)(η^5-cyclopentadienyl) ferrocene]] digold(I) (Me_2FOAu(I))**

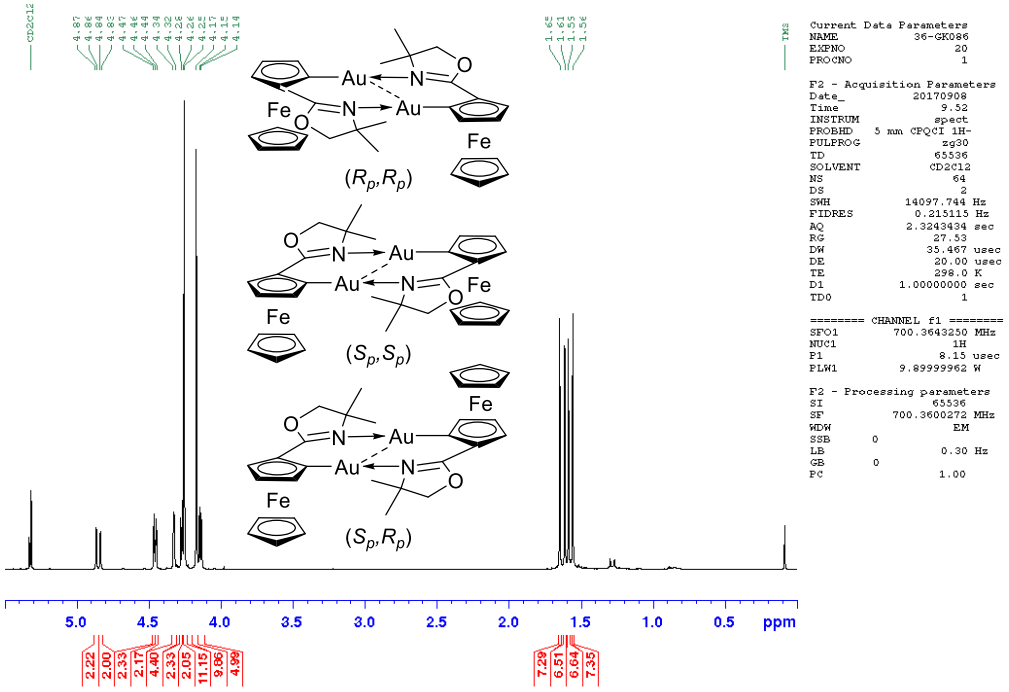

Figure S34 ^{1}H NMR spectrum at 700 MHz of Compound **Me_2FOAu(I)** in CD_2Cl_2.

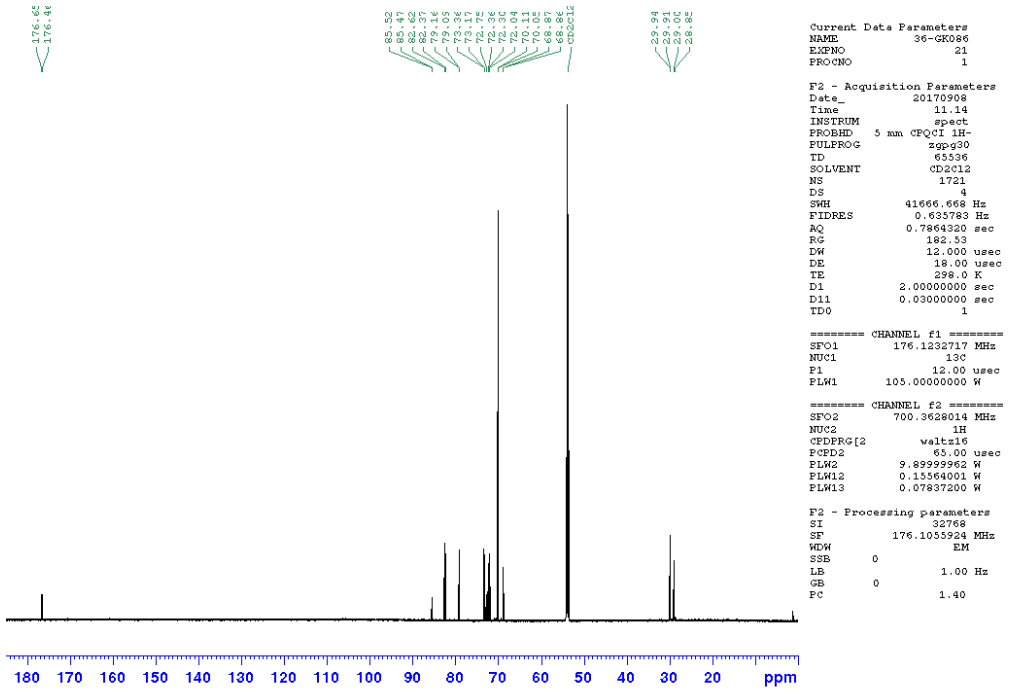

Figure S35 ^{13}C {^{1}H} NMR spectrum at 175 MHz of Compound **Me_2FOAu(I)** in CD_2Cl_2.

Dichlorobis[μ-[(η^5-(*S*,*R*$_p$)-2-(4'-isopropyl-4',5'-dihydro-2'-oxazolyl-κ*N*)-3-methyl-cyclopentadienyl-κ*C1*)(η^5-cyclopentadienyl) ferrocene]] digold(II) (*i*PrFOMeAu(II)Cl)

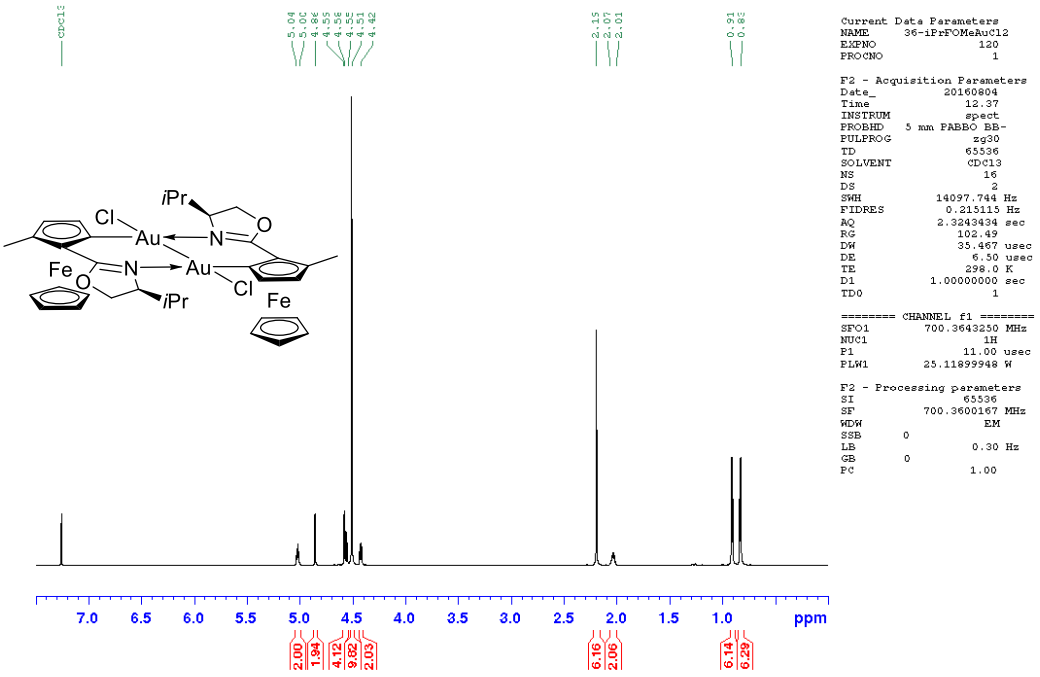

Figure S36 ^{1}H NMR spectrum at 700 MHz of Compound ***i*PrFOMeAu(II)Cl** in $CDCl_3$.

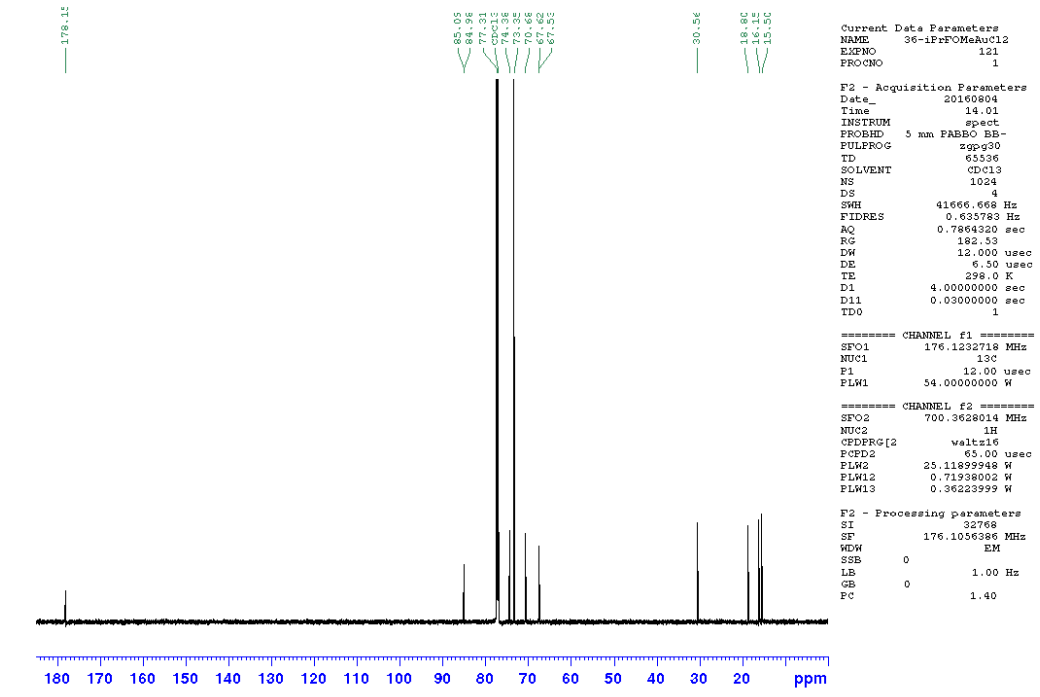

Figure S37 ^{13}C {^{1}H} NMR spectrum at 175 MHz of Compound ***i*PrFOMeAu(II)Cl** in $CDCl_3$.

Dichlorobis[μ-[(η^5-(*S*,*R*$_p$)-2-(4'-isopropyl-4',5'-dihydro-2'-oxazolyl-κ*N*)-3-trimethylsilyl-cyclopentadienyl-κ*C*)(η^5-cyclopentadienyl) ferrocene]] digold(II) (*i*PrFOTMSAu(II)Cl)

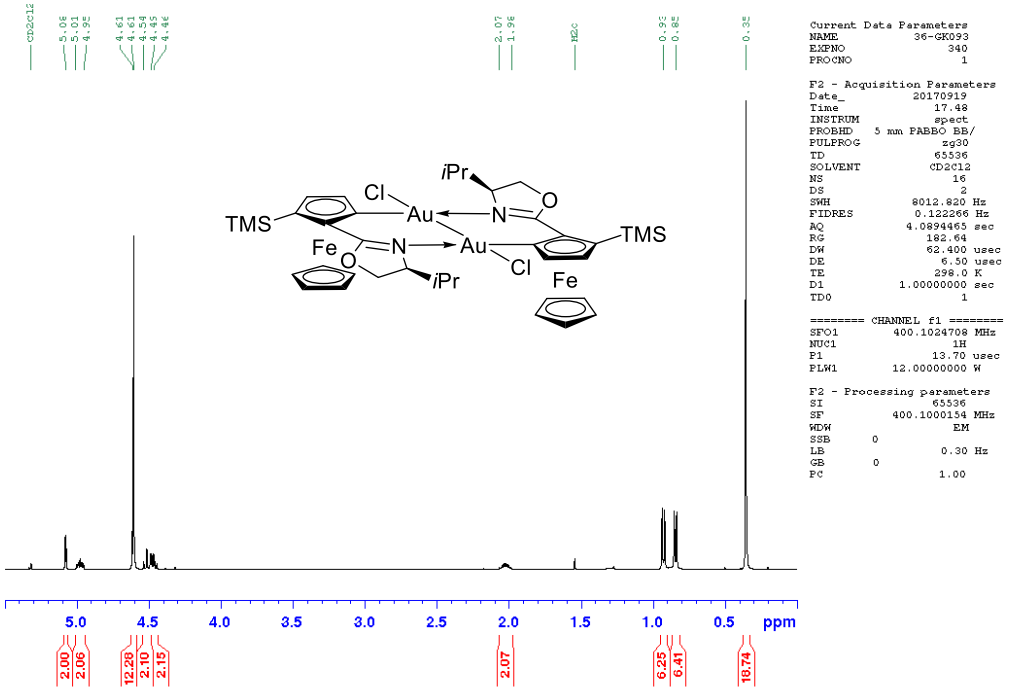

Figure S38 ^{1}H NMR spectrum at 400 MHz of Compound ***i*PrFOTMSAu(II)Cl** in CD_2Cl_2.

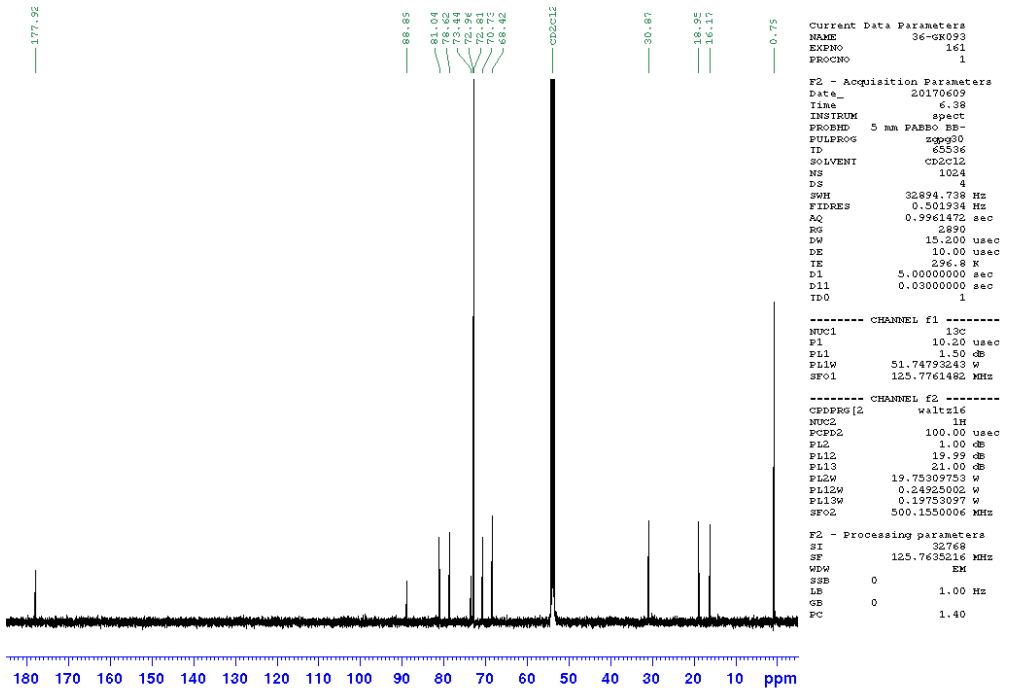

Figure S39 ^{13}C {^{1}H} NMR spectrum at 125 MHz of Compound ***i*PrFOTMSAu(II)Cl** in CD_2Cl_2.

Dichlorobis[μ-[(η^5-(*S*,*R*$_p$)-2-(4'-*tert*-butyl-4',5'-dihydro-2'-oxazolyl-κ*N*)-3-methyl-cyclopentadienyl-κ*C*)(η^5-cyclopentadienyl) ferrocene]] digold(II) (*t*BuFOMeAu(II)Cl)

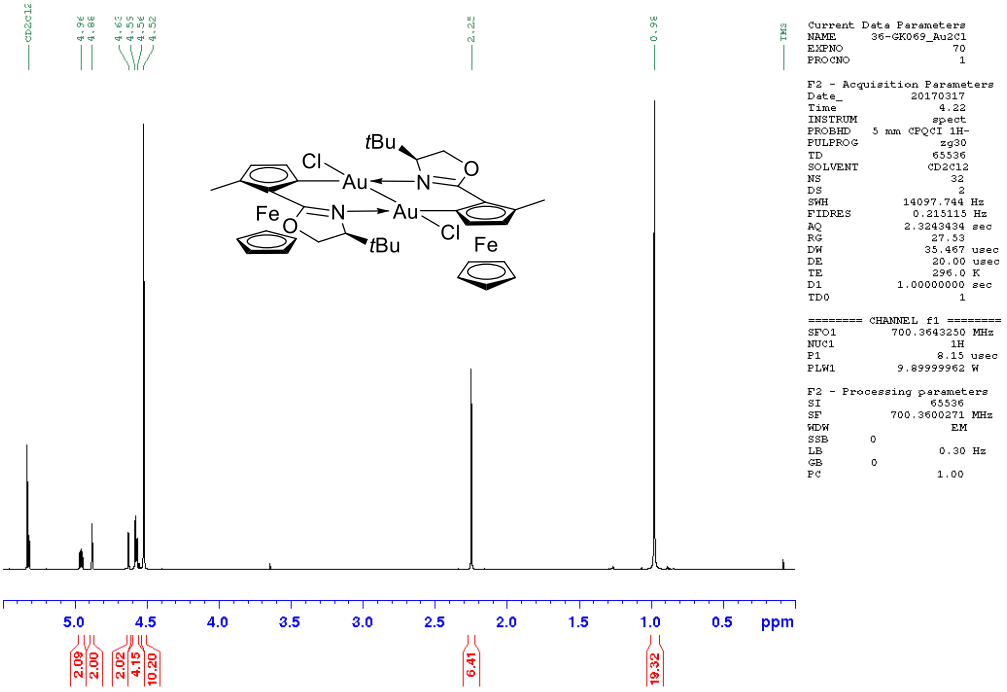

Figure S40 ^{1}H NMR spectrum at 700 MHz of Compound ***t*BuFOMeAu(II)Cl** in CD_2Cl_2.

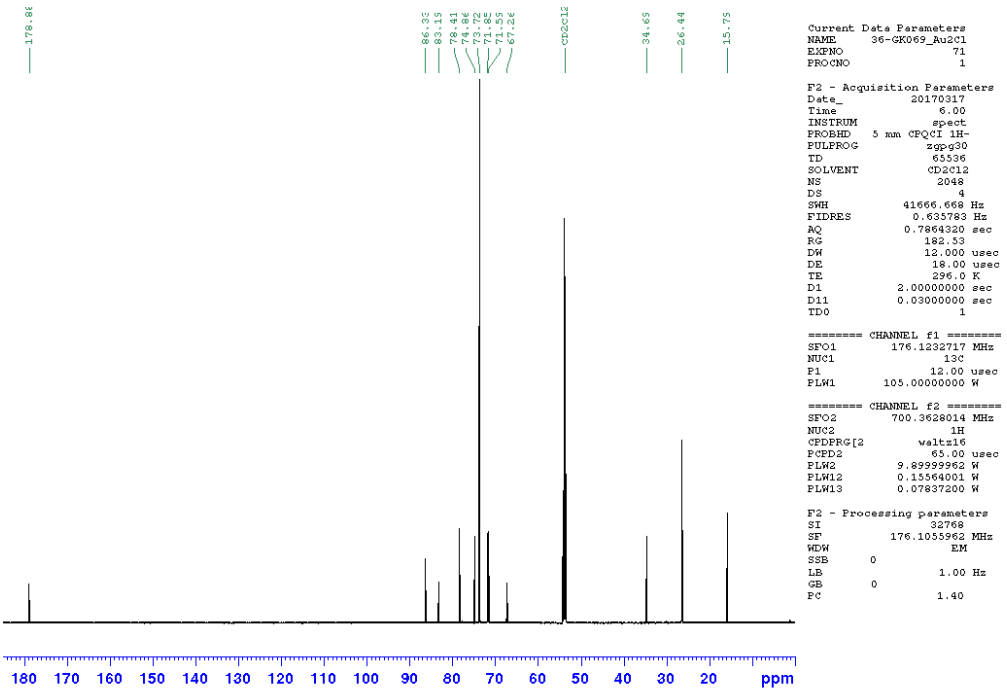

Figure S41 ^{13}C {^{1}H} NMR spectrum at 175 MHz of Compound ***t*BuFOMeAu(II)Cl** in CD_2Cl_2.

Dichlorobis[μ-[(η^5-(*S*,*S*$_p$)-2-(4',5'-5'*H*-Indeno[1,2-*d*]-4',5'-dihydro-2'-oxazolyl-κ*N*)-3-methyl-cyclopentadienyl-κ*C*)(η^5-cyclopentadienyl) ferrocene]] digold(II) (IndFOMeAu(II)Cl)

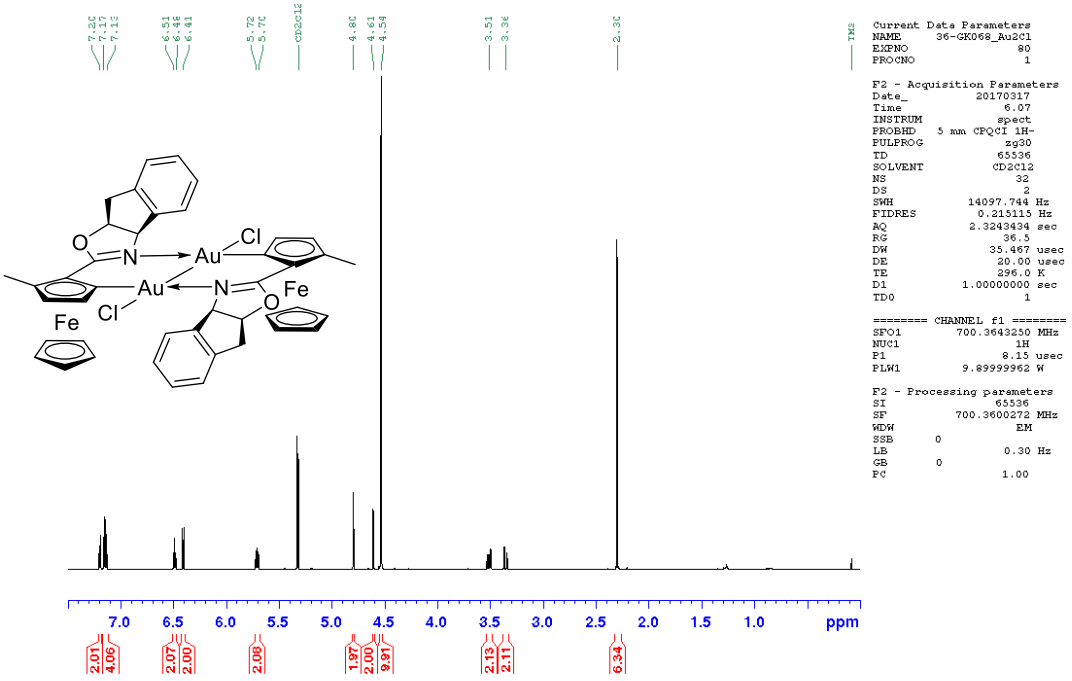

Figure S42 ^{1}H NMR spectrum at 700 MHz of Compound **IndFOMeAu(II)Cl** in CD_2Cl_2.

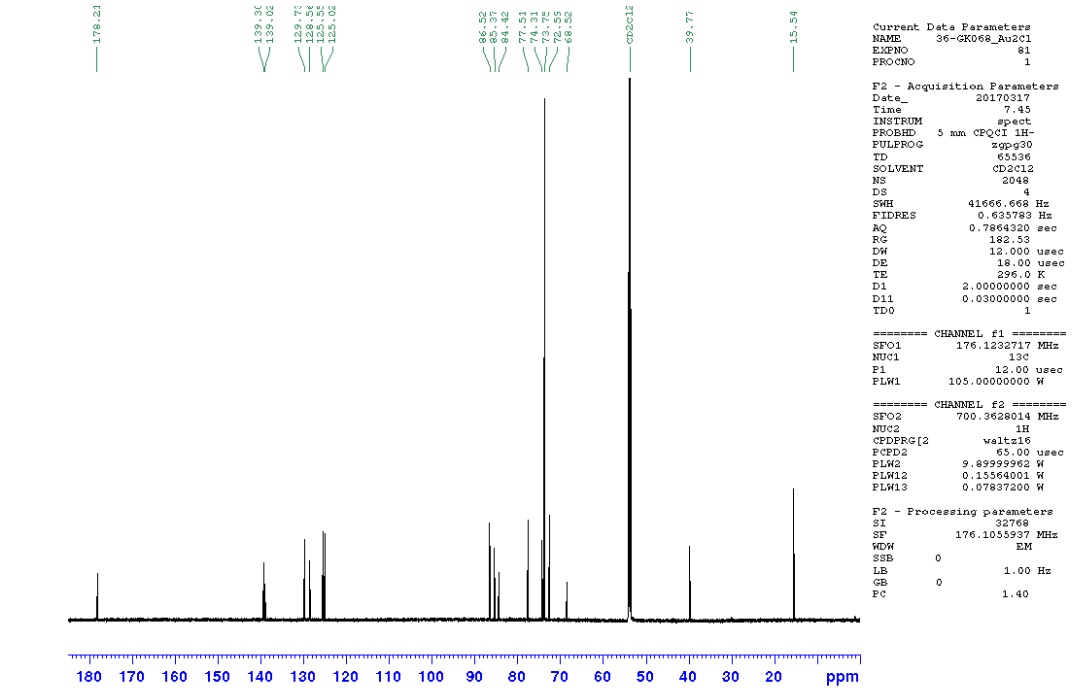

Figure S43 ^{13}C {^{1}H} NMR spectrum at 175 MHz of Compound **IndFOMeAu(II)Cl** in CD_2Cl_2.

Dichlorobis[μ-[(η^5-(*S*,*S*$_p$)-2-(4',5'-diphenyl-4',5'-dihydro-2'-oxazolyl-κ*N*)-3-methyl-cyclopentadienyl-κ*C*)(η^5-cyclopentadienyl) ferrocene]] digold(II) (Ph$_2$FOMeAu(II)Cl)

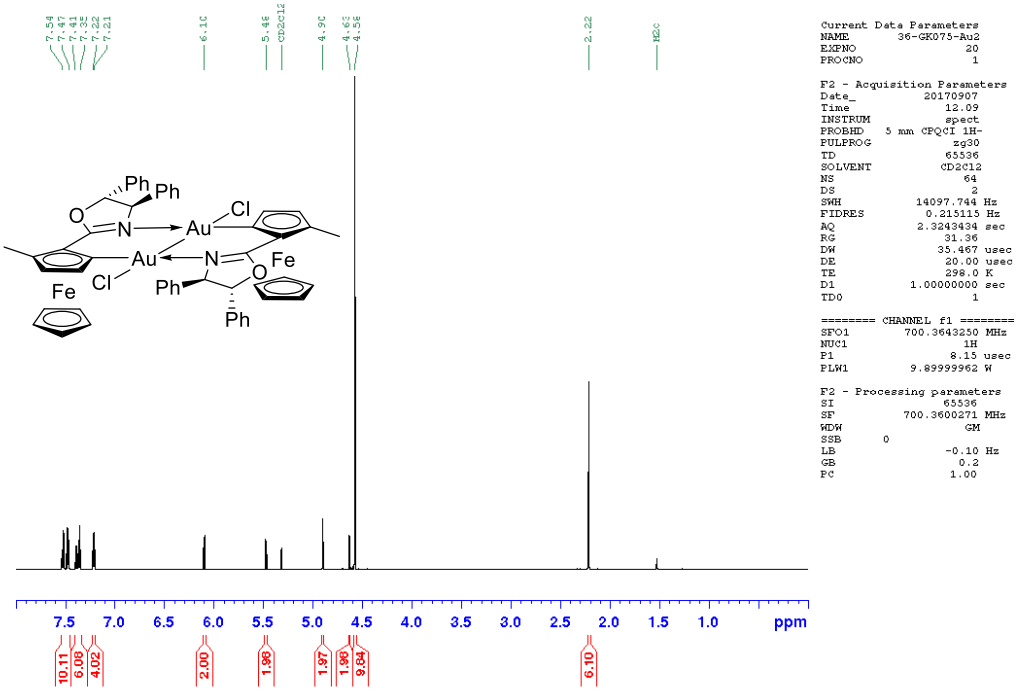

Figure S44 ^{1}H NMR spectrum at 700 MHz of Compound **Ph$_2$FOMeAu(II)Cl** in CD_2Cl_2.

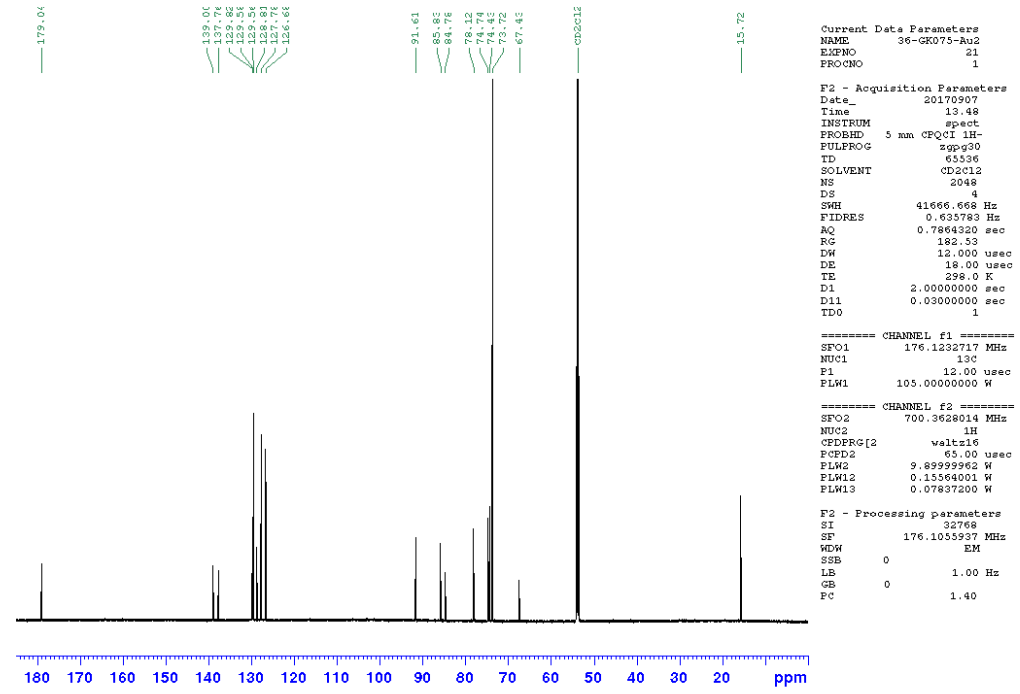

Figure S45 ^{13}C {^{1}H} NMR spectrum at 175 MHz of Compound **Ph$_2$FOMeAu(II)Cl** in CD_2Cl_2.

Dibromobis[μ-[(η^5-(*S*,*R*$_p$)-2-(4'-isopropyl-4',5'-dihydro-2'-oxazolyl-κ*N*)-3-methyl-cyclopentadienyl-κ*C1*)(η^5-cyclopentadienyl) ferrocene]] digold(II) (*i*PrFOMeAu(II)Br)

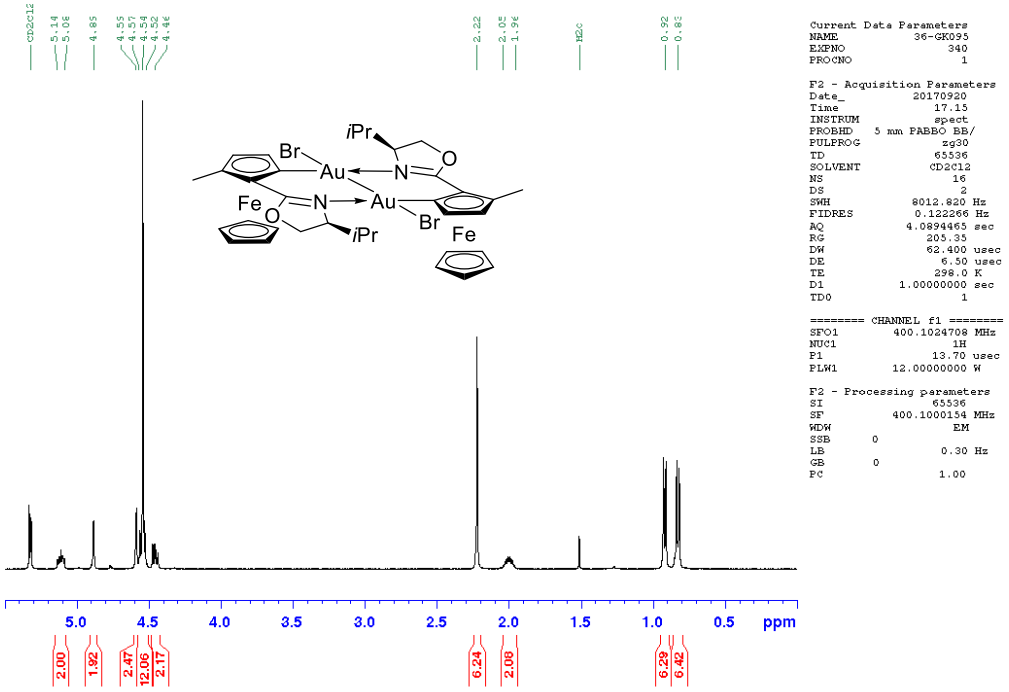

Figure S46 ^{1}H NMR spectrum at 400 MHz of Compound ***i*PrFOMeAu(II)Br** in CD_2Cl_2.

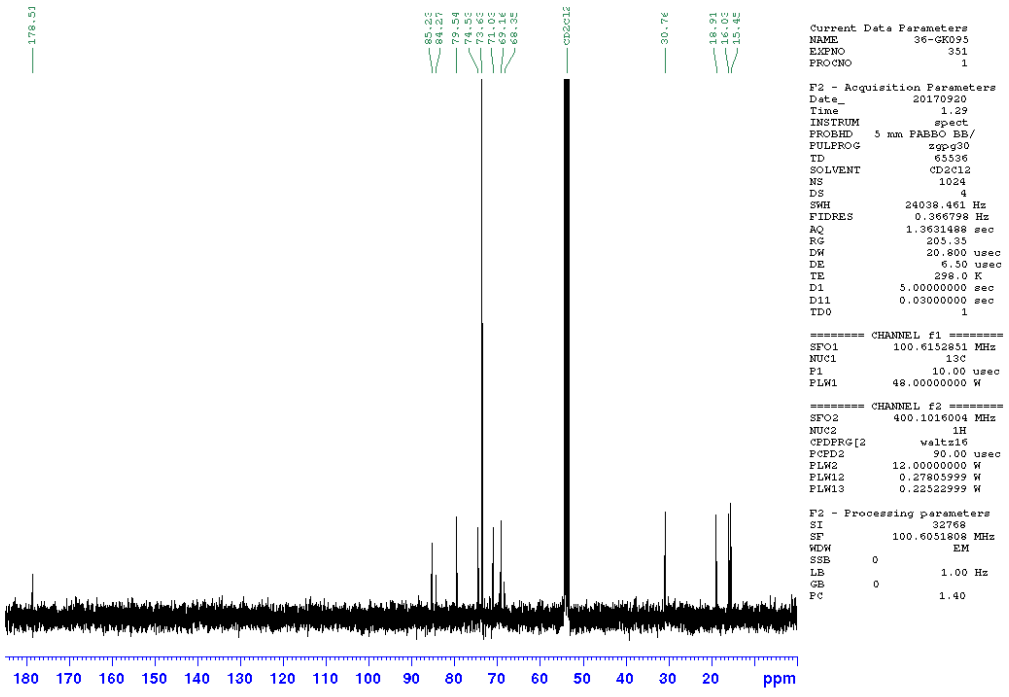

Figure S47 ^{13}C {^{1}H} NMR spectrum at 100 MHz of Compound ***i*PrFOMeAu(II)Br** in CD_2Cl_2.

Diiodobis[μ-[(η^5-(*S*,*R*$_p$)-2-(4'-isopropyl-4',5'-dihydro-2'-oxazolyl-κ*N*)-3-methyl-cyclopentadienyl-κ*C1*)(η^5-cyclopentadienyl) ferrocene]] digold(II) (*i*PrFOMeAu(II)I)

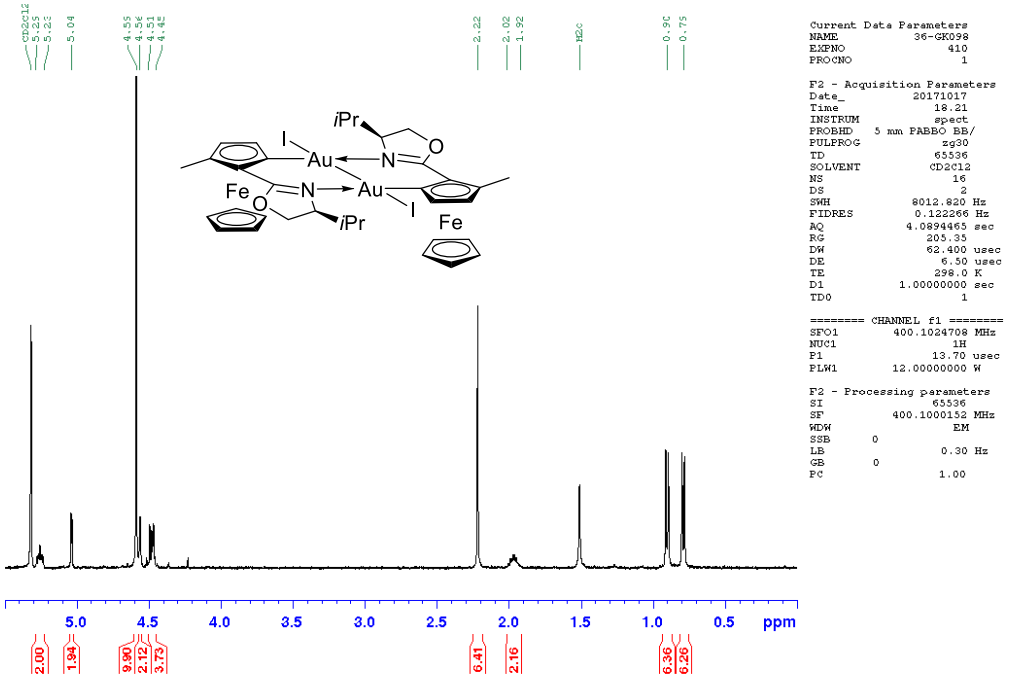

Figure S48 ^{1}H NMR spectrum at 400 MHz of Compound ***i*PrFOMeAu(II)I** in CD_2Cl_2.

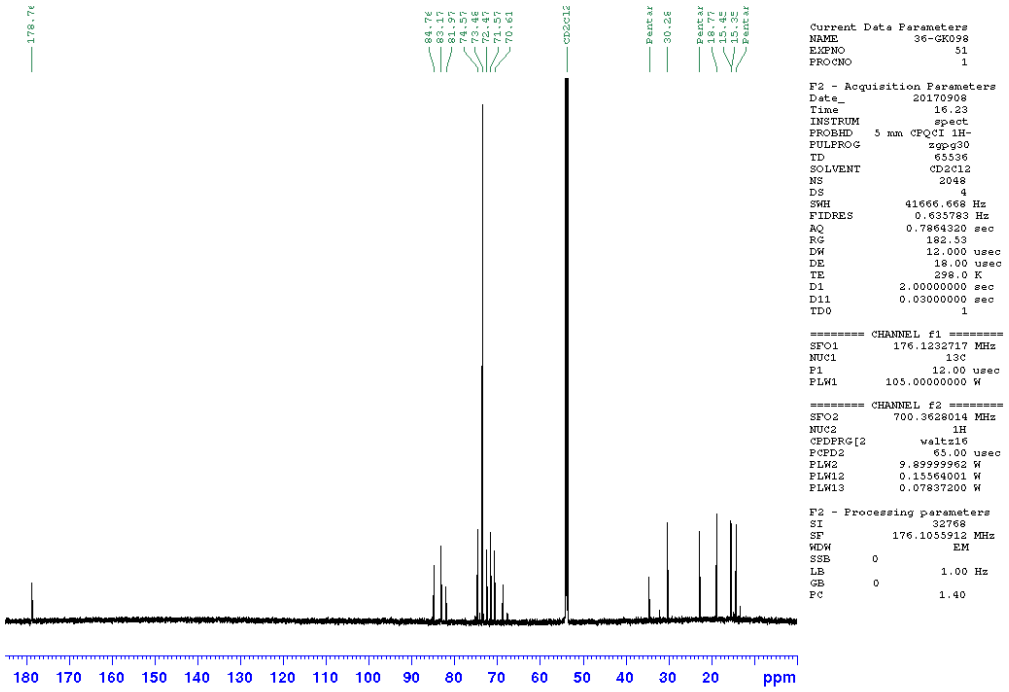

Figure S49 ^{13}C {^{1}H} NMR spectrum at 175 MHz of Compound ***i*PrFOMeAu(II)I** in CD_2Cl_2.

(*S*,R_p,*S*,R_p)-2,2'-Bis[(4-Isopropyl-4,5-dihydro-2-oxazolyl)-3-methyl] 1,1'-biferrocenyl ((*i*PrFOMe)$_2$)

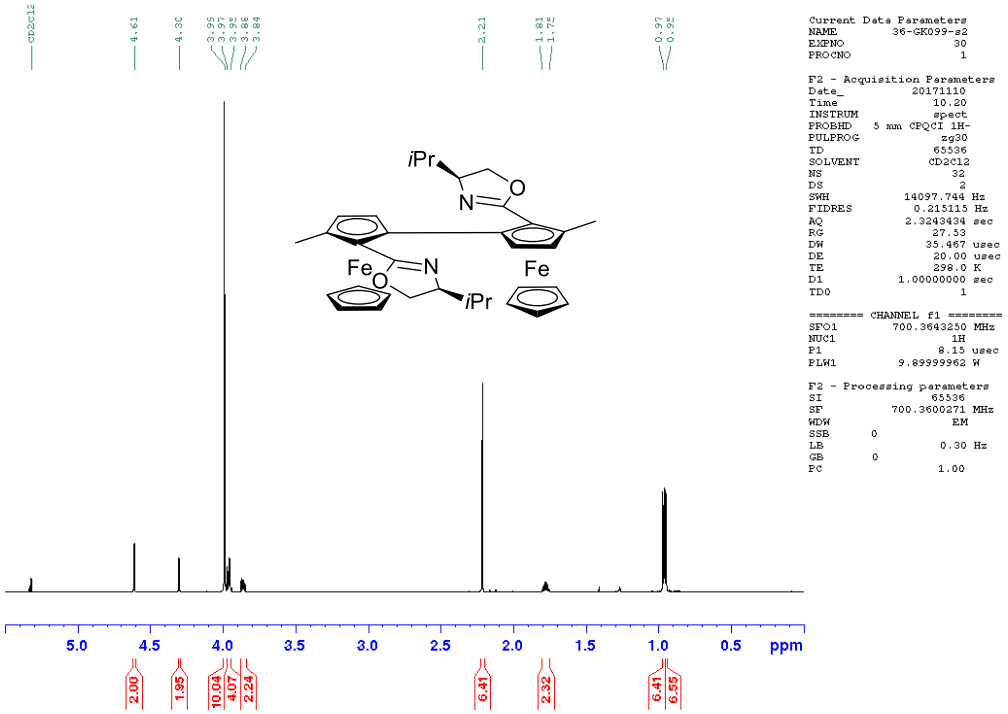

Figure S50 ^{1}H NMR spectrum at 700 MHz of Compound **(*i*PrFOMe)$_2$** in CD_2Cl_2.

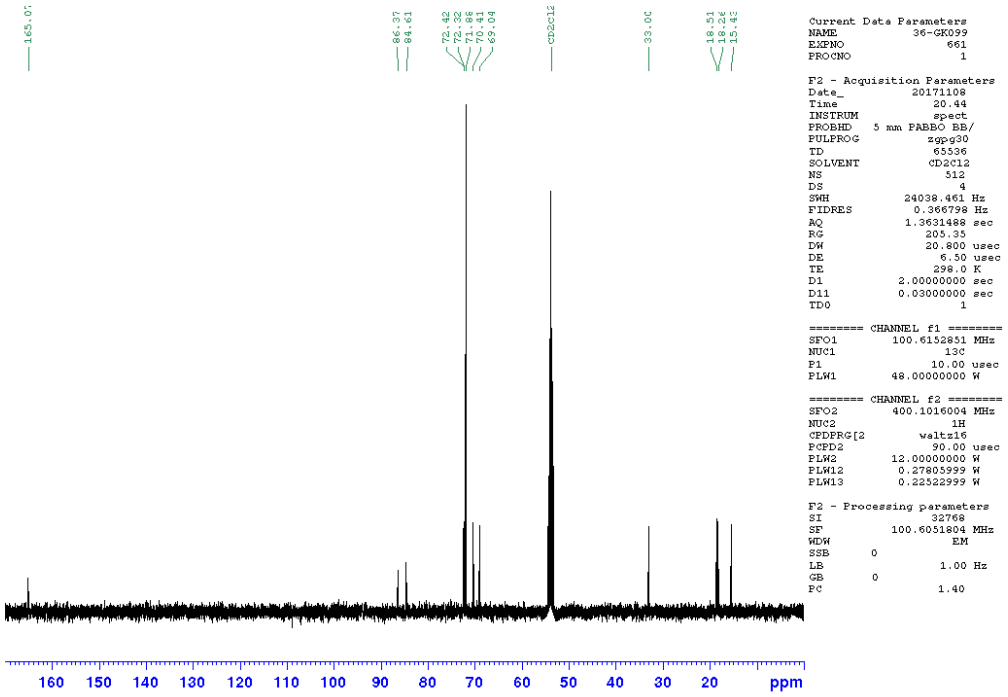

Figure S51 ^{13}C {^{1}H} NMR spectrum at 100 MHz of Compound **(*i*PrFOMe)$_2$** in CD_2Cl_2.

Diacetatobis[μ-[(η^5-(*S*,*R*$_p$)-2-(4'-isopropyl-4',5'-dihydro-2'-oxazolyl-κ*N*)-3-methyl-cyclopentadienyl-κ*C1*)(η^5-cyclopentadienyl) ferrocene]] digold(II) (*i*PrFOMeAu(II)OAc)

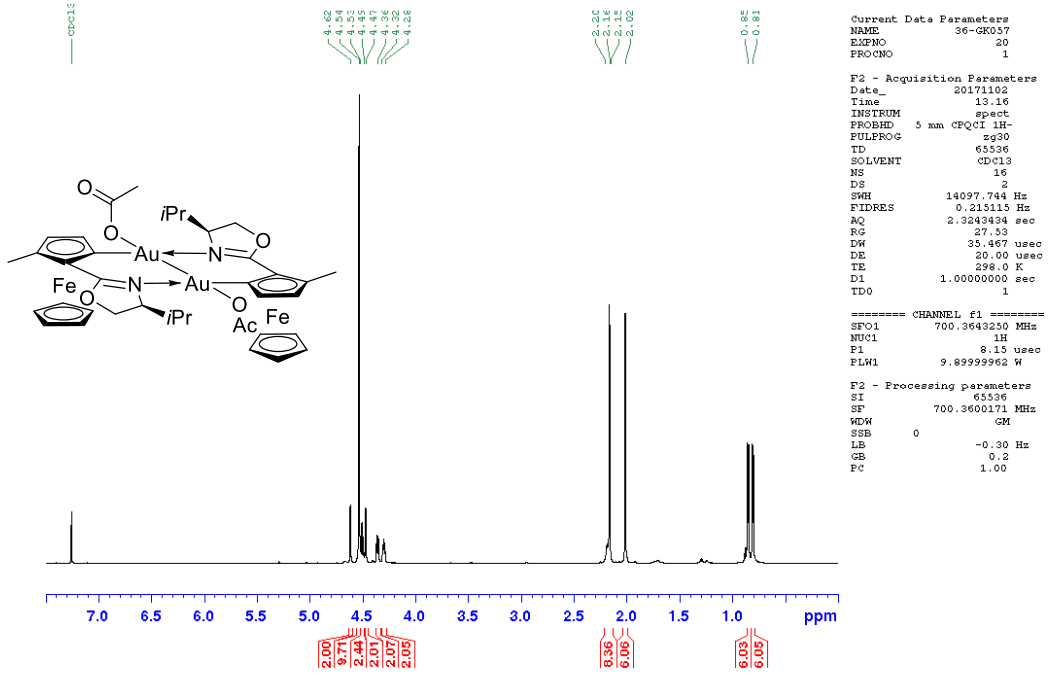

Figure S52 ^{1}H NMR spectrum at 700 MHz of Compound ***i*PrFOMeAu(II)OAc** in $CDCl_3$.

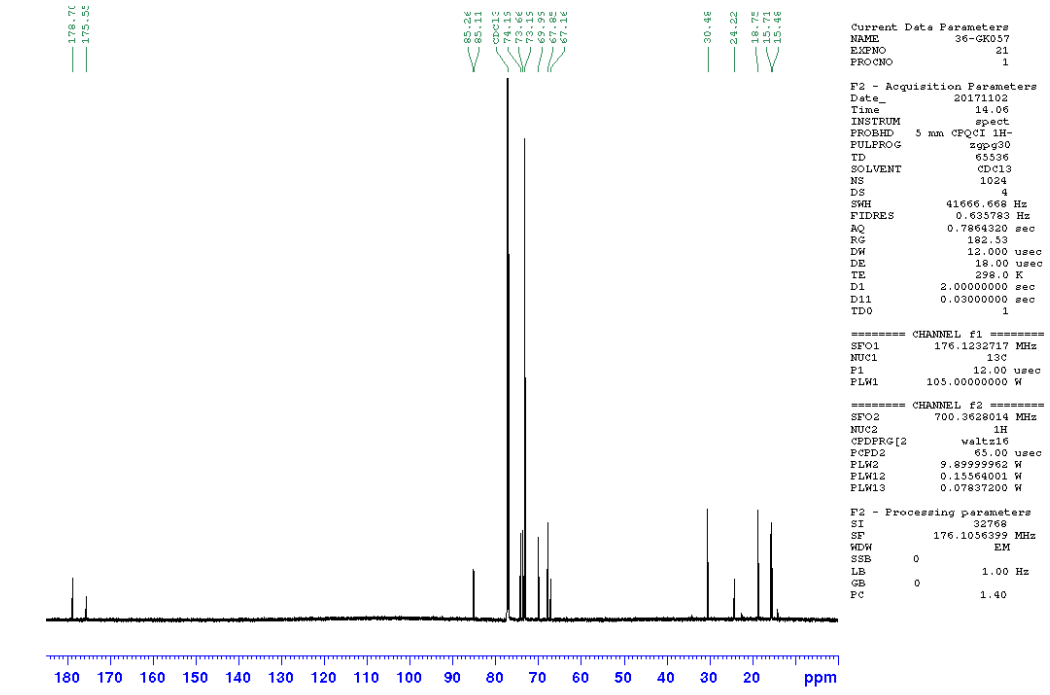

Figure S53 ^{13}C {^{1}H} NMR spectrum at 175 MHz of Compound ***i*PrFOMeAu(II)OAc** in $CDCl_3$.

UV-Vis Spectra

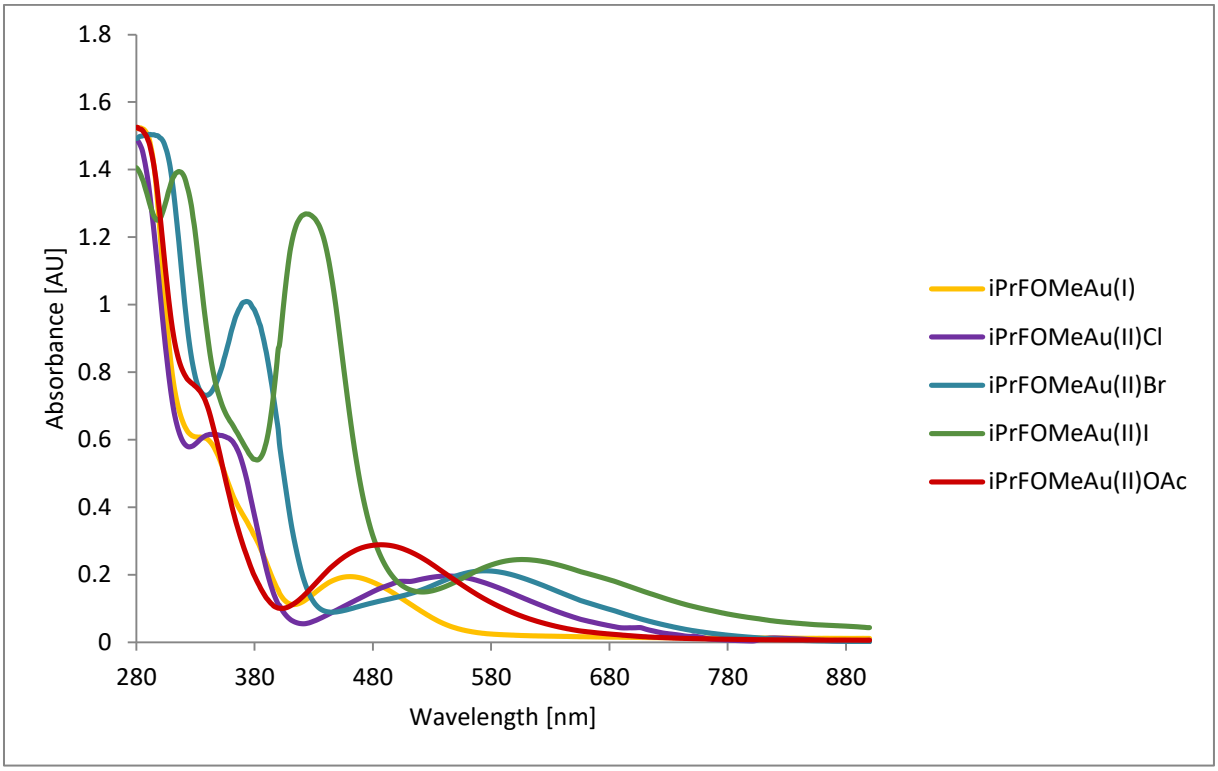

Figure S54 UV-Vis-Absorbance spectra for Au-complexes derived from ligand ***i*PrFOMe**.

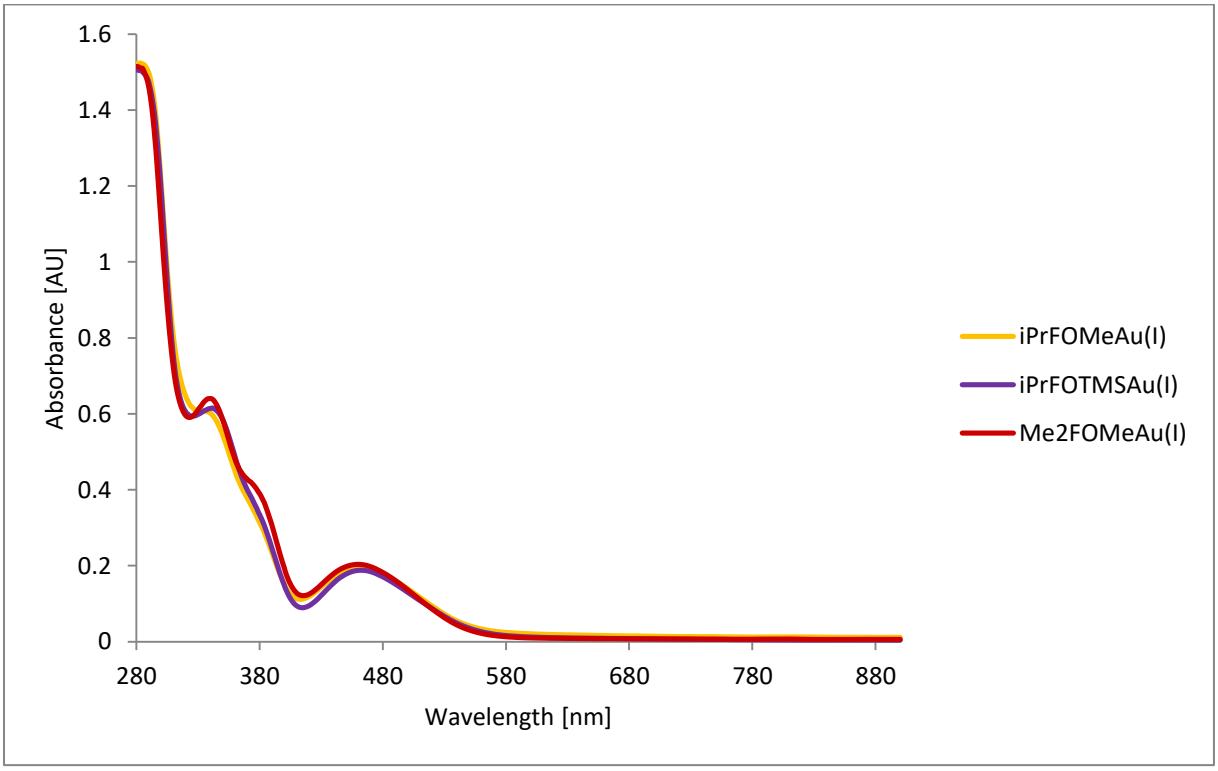

Figure S55 UV-Vis-Absorbance spectra of Au(I) complexes with different ligands.

CD-Spectra

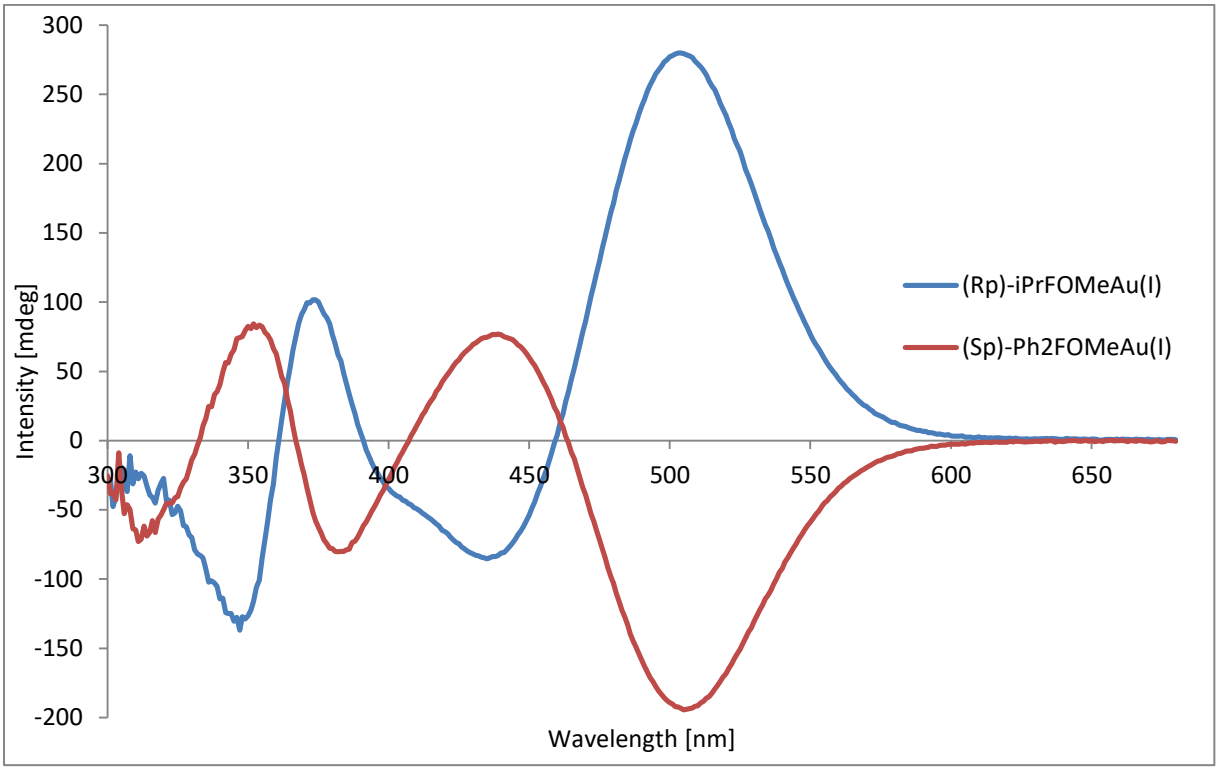

Figure S56 CD-spectra for Au(I)-complexes (concentrations used: (R_p)-*i*PrFOMeAu(I): 0.89 mmol/L; (S_p)-Ph_2FOMeAu(I): 0.49 mmol/L).

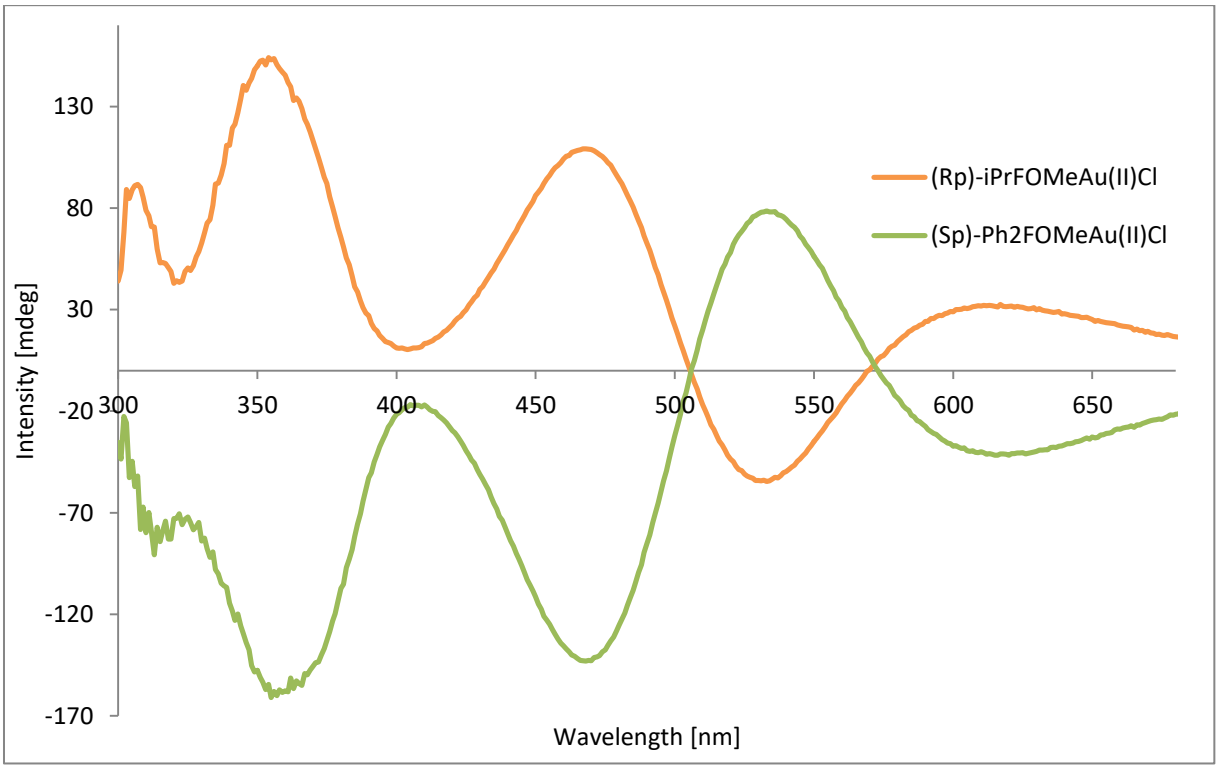

Figure S57 CD-spectra for Au(II)-complexes (concentrations used: (R_p)-*i*PrFOMeAu(II)Cl: 0.27 mmol/L; (S_p)-Ph_2FOMeAu(II)Cl: 0.27 mmol/L).